Characterizing the determinants of leaf patterning in maize

by

Dylan Cole Oates

MASTER OF SCIENCE

Major: Tropical Plant and Soil Sciences

Program of Study Committee:
Michael G. Muszynski
Michael Kantar
Clifford Morden

University of Hawai'i at Mānoa

Honolulu, Hawai'i

2019

ABSTRACT

Patterned growth is essential for proper plant development. However, the identity of the molecular signals that contribute to patterning remains incomplete. The maize leaf presents an excellent opportunity to study patterning due to its simplicity. The maize leaf is organized into four distinct tissues that are polarized in a proximal-distal (P-D) pattern: (1) sheath is the most proximal and wraps around the culm of the plant, (2) auricle and (3) ligule creating a hinge like structure that allows the leaf to bend away from the plant, and (4) blade is the most distal and acts as the main photosynthetic apparatus. I used the semi-dominant mutant *Hairy sheath frayed1* (*Hsf1*) to identify the molecular signals that influence leaf patterning.

The *Hsf1* mutant develops abnormal ectopic outgrowths on the blade margin, called “prongs”, consisting of proximal tissue in the most distal compartment of the leaf. Thus, *Hsf1* mutants have altered P-D leaf patterning. Map based cloning revealed that the *Hsf1* phenotype is a result of gain-of-function missense mutations in the CHASE domain of the *Zea mays Histidine Kinase1 (ZmHK1)* gene. *ZmHK1* encodes one of five cytokinin (CK) receptor proteins that perceive and signal the hormone CK. In the *Hsf1* mutant, *ZmHK1* has higher CK affinity compared to the wild-type, and CK responsive genes are upregulated. Moreover, the *Hsf1* phenotype can be phenocopied by exogenous CK treatments on wildtype inbred seeds. The picture emerging is that the *Hsf1* mutation causes too much CK signaling (hypersignaling) in developing leaves leading to altered P-D leaf patterning. This indicates CK signaling influences P-D leaf patterning, highlighting a new function for CK.

To identify the downstream determinants of CK signaling that drive prong formation, we used laser-capture microdissection (LCM) coupled with whole transcriptome sequencing (RNA-seq), on initiating prongs (P), no-prong (N, WT margin in *Hsf1*), and wild-type (W) margin tissue. Approximately 900 differentially expressed (DE) genes were identified that were enriched for transcription factors (TFs) associated with certain developmental processes. Based on these results, we hypothesized that CK hypersignaling causes blade margin cells to become dedifferentiated, assume a meristematic state, and initiate new primordia. This results in the generation of “newly formed leaves” with proximal identity along the distal blade margin.

Although the determinants of CK perception and signaling have been well defined in plants, the identity and function of downstream components are not well understood. **This thesis project is focused on determining the function of seventeen DE TFs, by genetics and genomics approaches, along with characterization of a new possible genetic enhancer of *Hsf1, enh*.** Histological methods were used on margin tissue to determine the prong developmental hallmarks based on normal leaf patterning. This led to the identification of three stages of prongs development, (1) emerging, (2) transitioning, and (3) mature. Quantitative PCR was used to determine the relative expression of seventeen genes of interest over each prong stage along with wild-type and no-prong margin. The relative expression and known gene function were compared to the previous RNA-seq data which revealed that not all genes were expressed in their predicted stages. Double mutant analysis of *Hsf1*/+ and *delayed flowering1* (*dlf1*) provided evidence for a function of *dlf1* in leaf development as described in objective 1. In the process creating *Hsf1*/+ and *tru1* double

mutants I uncovered a possible genetic enhancer of *Hsf1* in the A619 inbred background. Further analysis will need to be done to determine the underlying gene to the mutation.

ACKNOWLEDGEMENTS

I would like to thank my advisor, Dr. Michael G. Muszynski, for his mentorship, advice, and guidance throughout my graduate experience. He has taught valuable lessons in research and in professional fields of science, from which I have learned that “any chance to collect data is important”. His guidance through the getting this degree process is appreciated.

I am also grateful to Dr. Angel Del Valle Echevarria for his unyielding assistance and offering his experimental expertise in the field of molecular genetics. I would not have been able to make the progress I had without him. I would like to also thank the other members of the Plant Growth and Development lab for their various help in data collection and plant maintenance.

Lastly, I would like to extend my gratitude to my friends and family. Without their support, I do not believe I would have the drive or desire to continue pursuing my professional education. Without a doubt, they most certainly made the “tough” experiences bearable and possible to overcome.

Again, “Mahalo nui loa” and “A hui hoa”!

-Dylan Oates

Table of Contents

Table of Contents

LIST OF TABLES

phenotype. Last two columns are the calculated p-values for a 1:1 and 3:1 (standard: enhanced) *Hsf1* segregation ratio. Standard confidence; $P \leq 0.05$. WT, wild-type; Sta., Standard *Hsf1*; Enh., Enhanced *Hsf1.*

LIST OF FIGURES

ABBREVIATIONS

abph1	*aberrant phyllotaxy1*
CK	Cytokinin
DE	Differentially Expressed
dlf1	*delayed flowering1*
EMS	Ethyl methanesulfonate
HKs	Histidine kinases
HPts	Histidine phosphotransfer proteins
Hsf1	*Hairy sheath frayed1*
Kn1	*Knotted1*
knox	*knotted1-like homeobox*
lg3	*liguleless3*
LM	Laser Microdissection
P-D	Proximal-Distal
P1	Plastochron 1
PGR	Plant Growth Regulators
RRs	Response Regulators
TF	Transcription Factor
tru1	*tassel replaces upper ear1*
ZmHK1	*Zea mays Histidine Kinase1*

INTRODUCTION

Growth and development

Development from a single fertilized embryo to a mature plant follows a precise and highly organized succession of events. Development, not to be confused with differentiation, is considered an umbrella term that refers to the sum of all the biological changes that a cell, tissue, organ, or organism goes through in its life cycle (Hopkins & Hüner, 2008). Morphological changes are visibly manifest in an organ or an organism, such as the transition from; a seed to a seedling, a leaf primordium to a mature leaf, or the vegetative to reproductive state. These transitions are well characterized, but the molecular signals that control these developmental changes are often incomplete. (Hopkins & Hüner, 2008). Understanding these developmental mechanisms are important to in order to have a more complete picture of how the plant progresses through its life cycle.

Growth is defined as the irreversible gain of biomass due to cellular division and elongation (Hopkins & Hüner, 2008). Cell division and cell enlargement are separate events. It is known that cell division can occur without growth (Borzouei, Kafi, Khazaei, Naeriyan, & A.Majdabadi, 2010; MacArthur & D'Appolonia, 1984; Pritchard, Pigden, & Minson, 1962). Growth can be quantitatively expressed through various techniques, such as leaf analyses, height, and yield.

Differentiation refers to the qualitative changes that follow growth (Hopkins & Hüner, 2008). This process occurs when cells assume their specialized function, allowing them to perform key roles in the plant physiology, metabolism, and development. Unique to plants, differentiation is reversible. Cells with specialized

function can revert to an undifferentiated state. This can be seen in tobacco or soybeans, when cells isolated from the stem or cotyledons are cultured on artificial media to produce callus tissue (Freytag, Rao-Arelli, Anand, Wrather, & Owens, 1989; Sacristan & Melchers, 1969). Understanding these three terms will be essential to understanding the research discussed in this thesis.

Maize Leaf Development

Leaf development initiates when the leaf primordia emerges from the shoot apical meristem (SAM). In the mature quiescent maize embryo, there are approximately four to five leaf primordia that flank the SAM (Zimmermann & Werr, 2005). Each of these leaf primordia are marked by different developmental stages and are denoted by plastochron number. The leaf primordia closest to the SAM is the most recently initiated and is referred to as plastochron 1, or P1. The outer most leaf is the oldest and will be the first to emerge from the coleoptile after germination [Figure 1].

Class I KNOTTED1-LIKE HOMEOBOX (KNOX) transcription factors, along with multiple phytohormones, are involved in the initiation and development of leaves (Hareven, Gutfinger, Parnis, Eshed, & Lifschitz, 1996; Ramirez, Bolduc, Lisch, & Hake, 2009; Townsley et al., 2013). Class I KNOX proteins function to maintain the totipotent nature of meristem cells and are down regulated at the site of initiating leaf primordia (P0). In *Arabidopsis*, KNOX proteins have been shown to activate cytokinin biosynthesis and decrease gibberellic acid accumulation, providing evidence of interactions, or crosstalk, between naturally occurring hormones to maintain meristem activity (Yanai et al., 2005). Recent discoveries in rice and maize have provided further evidence that

KNOX proteins are key regulators underlying meristem maintenance and their ectopic expression also affects leaf patterning (Toriba et al., 2019).

As leaves mature, their cells will undergo division, elongation, and maturation. The maize leaf can be divided into three specialized zones: (1) cell division, (2) cell elongation, and (3) cell maturation (Johnston et al., 2014). Cell division occurs at the most proximal compartment, where cells are produced, leading to the region of youngest cells. Mature cells are at the most proximal end of the leaf, where they have a specialized function. Between dividing and mature cells, cell size and shape change without increasing cell number, because cells are elongating.

A mature maize leaf is comprised of four distinct tissues that are polarized in the proximal-distal (P-D) axis; sheath, auricle, ligule, and blade [Figure 2]. The sheath is the most proximal, which wraps around the culm, while the blade is the most distal tissue and is used for photosynthesis. Both segments are separated by an auricle and a ligule, which create the hinge-like structure that allows the blade to bend away from the stalk (Lewis et al., 2014; Richardson & Hake, 2018) [Figure 2]. How this P-D leaf pattern initiates and is maintained during leaf development are still largely unresolved.

Leaf Patterning Genes

The class I KNOX genes *KNOTTED1* (*KN1*), *LIGULELESS3* (*LG3*), and *ROUGHSHEATH1* (RS1) have been shown to play a role in leaf patterning in maize (Kessler & Sinha, 2004; Moon, Candela, & Hake, 2013; Muehlbauer et al., 1999; Veit et al., 1993). The gain-of-function *knotted1* mutant, *Kn1-DL*, ectopically expresses KNOTTED1 in the distal most compartments of the blade, resulting in normally proximally located sheath-like tissue emerging from the margins (Ramirez et al., 2009).

This provides evidence that *KNOX* genes can cause a disruption of the spatial recognition of cells and tissues polarized along the P-D axis in leaf patterning. Recently, rice homologs of the *Arabidopsis BLADE-ON-PETIOLE1* (*BOP1*) gene, the OsBOPs, have been shown to be key determinants of leaf sheath identity that regulate the blade-sheath ratio (Toriba et al., 2019).

KNOX genes have been shown exert their function through modulation of specific hormone levels, such as CK. The loss-of-function maize mutant, *aberrant phyllotaxy1* (*abph1*), causes an altered phyllotaxy or leaf arrangement, , where instead of a single leaf at every node, there are two leaves in the *abph1* mutants, but no leaf patterning phenotypes (Scanlon, Schneeberger, Freeling, & Jurgens, 1996). It was shown that the underlying gene for the *abph1* phenotype is type-A RR, *Zea mays RESPONSE REGULATOR3* (*ZmRR3*), which is a negative regulator of CK signaling and a positive regulator of auxin (Giulini, Wang, & Jackson, 2004).

Plant Growth Regulators (PGR)

Plant hormones, also known as phytohormones or plant growth regulators (PGRs), are signal molecules that control many aspects of plant growth and development. These naturally produced compounds are locally synthesized at low concentrations and are transported to their appropriate target tissue where they elicit a biological response (Atwell, Kriedemann, & Turnbull, 1999). There are currently nine essential hormones that have been: abscisic acid (ABA), auxin (IAA), brassinosteroids (BR), cytokinin (CK), ethylene (ET), gibberellin (GA), jasmonic acid (JA), salicylic acid (SA), and strigolactones (SL) (Hopkins & Hüner, 2008). The biosynthesis, conjugation, and catabolism have been well described for each of these PGRs, as well as their

biological effects on physiology, growth and development, such as CK [Figure 4]. PGRs are known to interact with one another in control of a biological process, which is termed “crosstalk”, and current work has been aimed at identifying the molecular players which facilitate the crosstalk (Chandler & Werr, 2015; Liu, Moore, Chen, & Lindsey, 2017; Sankar et al., 2011; Schaller, Bishopp, & Kieber, 2015).

Cytokinin

Cytokinin (CK) is a phytohormone that is associated with regulating cell proliferation and differentiation such as delaying cell fate or senescence (Pilkington et al., 2013; Rodo et al., 2008; Skalák et al., 2019). Initially discovered by Drs. Folk Skoog and Carlos Miller in the 1950s, it was first isolated as an unknown active compound from autoclaved Herring sperm. This adenine derivative, N^6-furfurylaminopurine, was shown to influence cellular proliferation in tobacco tissue cultures (SKOOG & MILLER, 1957). Later, the molecule kinetin was identified as a cytokinin due to its role in cell division (cytokinesis) (Hopkins & Hüner, 2008).

Biosynthesis, Conjugation, and Catabolism of Cytokinin

CK naturally occurs as two adenine derived compounds forming either (1) isoprenoids or (2) aromatic molecules, with the former found more often (Chen, 1997; Sakakibara, 2006). Common isoprenoid CKs are N^6-(Δ^2-isopentenyl)- adenine (iP), *trans*-zeatin (tZ), *cis*-zeatin (cZ), and dihydrozeatin (DZ) (Hopkins & Hüner, 2008; Sakakibara, 2006) [Figure 5]. The most biologically significant are iP and tZ, which were isolated from maize (*Zea mays*). Interestingly, iP and tZ are the major forms in dicots, while cZ and tZ are found in substantial amounts in monocots (D’Aloia et al., 2011;

Izumi et al., 1988; Letham, 1963; Li et al., 2011; Takagi, Yokota, Murofushi, Ota, & Takahashi, 1985; Takagi, Yokota, Murofushi, Saka, & Takahashi, 1989).

The biosynthesis of isoprenoid CKs are achieved by a two-pathway mechanism: the methylerythritol phosphate (MEP) pathway and mevalonate (MVA) pathway (Sakakibara, 2006). The MEP pathway occurs in plastids and is the first step in the biosynthesis of isoprenoid CK. Here, the N-prenylation of adenosine 5'-phosphates (AMP, ADP, or ATP) with either dimethylallyl diphosphate (DMAPP) or hydroxymethylbutenyl diphosphate (HMBDP) is catalyzed by phosphate-isopentenyltransferase (IPT) (Hopkins & Hüner, 2008; Sakakibara, 2006). When DMAPP is primarily used as the substrate results in the production of iP, while when HMBDP is used as the primary substrate, tZ is produced. The MVA pathway occurs in the cytosol and the hydroxylation of riboside 5'-monophosphate (iPRMP), iP riboside 5'-diphosphate (iPRDP), or iP riboside 5'-triphoshpate (iPRTP) is catalyzed via the action of CYP735A1 and CYP734A2 (P450 monooxygenases) into tZ and cZ CKs. Once the bioactive nucleobases are synthesized, they are perceived by CK-receptors and cause activation of downstream responses (Takei, Yamaya, & Sakakibara, 2004).

Steady-state levels of active CK are determined by conjugation and catabolism of CK nucleobases. Irreversible degradation of isoprenoid CKs can occur via CK oxidase/ dehydrogenase (CKX) by cleavage of the side chain (Schmülling, Werner, Riefler, Krupková, & Bartrina y Manns, 2003). Inactivation of CKs can occur through two types of glycosylation, permanently by *N*-glycosylation or temporarily by *O*-glycosylation (Sakakibara, 2006).

Translocation of CK

A major site of CK biosynthesis for most plants is in the roots where they are then transported to the foliar tissue through the xylem (Hopkins & Hüner, 2008; Sakakibara, 2006). CKs are mostly transported in their nucleoside forms with the assistance of the Equilibrative Nucleoside Transporter (ENT) protein family that are known to catalyze the transport of purines and nucleosides (Hopkins & Hüner, 2008; Sakakibara, 2006). CKs transported through the xylem allows for long-distance transport to targeted cells and tissues (Bishopp et al., 2011; Kang, Lee, Sakakibara, & Martinoia, 2017).

Perception and Signaling of CK

More than fifty years after Skoog and Miller isolated the first CK, it was only in the last two decades that the first receptor of CK was identified (Inoue et al., 2001). First discovered in *Arabidopsis*, several assays using hypocotyl sections and measuring their response to CK treatments led to the identification of *CYTOKININ RESPONSE1* (*CRE1*) as a CK receptor (Inoue et al., 2001). This same gene had also been identified by different labs as *WOODENLEG* (*WOL*) and *ARABIDOPSIS HISTIDINE KINASE4* (*AHK4*) (Inoue et al., 2001). Similar to *CRE1*, the maize cytokinin receptor *Zea Mays HISTIDINE KINASE1* (*ZmHK1*) receptor is a membrane-based histidine kinase (Sakakibara, 2006).

CK signaling occurs similar to the two-component signal transduction systems. Histidine kinase receptors (HKs) are autophoshporylated at the histidine kinase domain upon CK perception. Then, the phosphate group is transferred to the aspartate residue in the receiver domain of the HK receptor. The HK transfers this phosphate from the

receiver domain to a Histidine phosphotransfer protein (HPT). The phosphorylated HPTs transit between the cytosol and nucleus, where inside the nucleus the phosphate group is transferred to a Type-B Response Regulator (RR-B) protein, which are positive regulators of CK perception. The RR-Bs function as transcription factors and, after phosphorylation, bind to the promoter of CK responsive genes, to activate expression of downstream genes that mediate CK responses [Figure 6].

Biological Function: CKs are important regulators of growth and development

CK plays a major role in regulating cellular division. In tobacco cell cultures, the absence of CKs caused cells to arrest at the G2 phase of the cell cycle, while exogenous CK application overcame arrest allowing division to proceed (Zhang, Letham, & John, 1996). This result suggested that CKs promote division through interactions with cyclin-dependent kinases (CDK) that catalyze the dephosphorylation of the cyclin complex via a cytokinin-dependent phosphatase in cell division (Zhang et al., 1996).

Genetic studies have shown that CKs play a role in several critical developmental processes (Wybouw & De Rybel, 2019). CKs have been known to play regulatory roles in meristem maintenance in numerous species such as *Arabidopsis* (Dello Ioio et al., 2007; Gordon, Chickarmane, Ohno, & Meyerowitz, 2009; Leibfried et al., 2005; Moubayidin, Di Mambro, & Sabatini, 2009), rice (Kyozuka, 2007; Pautler, Tanaka, Hirano, & Jackson, 2013), maize (Pautler, Tanaka, Hirano, & Jackson, 2013) and mustard (Su, Liu, & Zhang, 2011). For example, in *Arabidopsis* transgenic lines that overexpress *CYTOKININ OXIDASE/ DEHYDROGENASE* (*CKX*), plant phenotypes display slowed shoot development, dwarfed, delayed flowering, and reduced shoot

apical meristem (Schmülling et al., 2003). Also, in the cytokinin-deficient rice mutant, *lonely guy* (*log*), panicle development was severely reduced (Han, Yang, & Jiao, 2014; Li et al., 2011). It was discovered that *LOG* encodes a phosphoribohydrolase that removes the ribose phosphate group from inactive CKs (Han et al., 2014; Li et al., 2011). As a consequence, the absence of *LOG* in mutants would decrease the levels of active CK, thus reducing cell division and hindering proper meristem maintenance. Since *LOG* is expressed in reproductive meristems, *log* mutant plants have smaller and fewer inflorescence branches containing fewer spikelets (Han et al., 2014; Li et al., 2011). An example of a CK mutant in maize is *aberrant phyllotaxy1* (*abph1*), where the arrangement of flowers and leaves along the rachis or stem (also known as phyllotaxy) are altered (Lee et al., 2009). It was found that *ABPH1* encodes for a CK-inducible type-A RR, and mutation of *abph1* resulted in a reduced SAM size, and altered auxin signaling, which changed phyllotaxy [Figure 8]. Although several CK mutants have been identified and studied in Arabidopsis, rice and other model plant species, there are only two CK mutations described for maize, *abph1* (*ZmRR3*) mentioned above and the *Hairy sheath frayed1* (*Hsf1*) mutation that is the subject of this thesis (Bertrand-Garcia & Freeling, 1991).

The *Hairy Sheath Frayed1* Mutant Affects Leaf Patterning and Growth

Hairy sheath frayed1 (*Hsf1*) is a semi-dominant gain-of-function mutant that effects maize leaf patterning in a specific manner (Bertrand-Garcia & Freeling, 1991; Saberman & Bertrand-Garcia, 1997). The term “frayed” refers to the abnormal ectopic proximal tissue, called prongs, that develops and grows from the distal blade margin which alters the proximal-distal (P-D) leaf pattern [Figure 7]. *Hsf1* mutants also have an

increased density of macrohairs on the sheath as well as the adaxial side of the blade. Mutant plants also grow slowly, producing shorter and narrower leaves compared to wild-type sibs. Even though the *Hsf1* prong phenotype looks similar to the *Knotted1* gain-of-function mutant, *Kn1-DL*, which also produces abnormal growths from the margin, it is not a *KNOX* gene (Ramirez et al., 2009). Map-base cloning of the *Hsf1* mutation revealed that *Zea mays HISTIDINE KINASE1* (*ZmHK1*), a CK receptor, as the gene underlying this mutant phenotype. The cause of the unique phenotypes was due to missense mutations in the CHASE binding domain of the *ZmHK1* receptor. These single amino acid changes in the CHASE domain result in a higher binding affinity for CK and, therefore, caused hypersignaling (Muszynski, et al., unpublished).

Exogenous application of CK to maize seeds phenocopies the *Hsf1* phenotype (Cahill, 2015). Since *Hsf1* mutants exhibit phenotypes that affect normal leaf patterning as a consequence of a hyperactive *ZmHK1*, this indicates that CK can influence leaf patterning. This is a new function for CK, as this hormone had not been shown to affect leaf patterning previously.

Unpublished data by Dr. Michael G. Muszynski et al. have identified CK responsive genes that may influence prong development and thus could be involved in leaf patterning. Utilizing laser-captured microdissection (LCM) tissue samples were collected from Hsf1 prong, and no-prong margins, and wild-type margins [Figure 9]. RNA-sequencing conducted on these three samples for four reps revealed thirty million reads per library. Alignment of these reads to the maize B73 genome identified approximately thirty-five thousand genes. Among these genes approximately eight hundred were found to be differentially expressed (DE) between the wild-type and prong

tissue. Gene ontology (GO) analysis revealed an enrichment of transcription factors (TFs), prominent among those were those with known or suspected functions in organogenesis. It was hypothesized that these DE TF genes had roles in producing the unique *Hsf1*/+ prong phenotype by acting downstream from the *ZmHK1* receptor. This laid the foundation to further define the functions of these DE genes and thus, gain insight into the determinants that influence leaf patterning. Seventeen genes were prioritized based on a number of criteria, including their fold change in the prong margin compared to the WT and no-prong tissue [Table 1]. The characterization of these 17 DE genes was the basis of my master's thesis research.

Figure Legends

Figure 1. Overview of a maize embryo with five leaf primordia. The outer most leaf is P5, which was the first primordium initiated from the shoot apical meristem (SAM), and will be the first to emerge from the coleoptile. The innermost leaf is the P1. It is the most recently initiated primordium, and is the leaf primordium closest to the SAM (Modified from Zimmermann & Werr, 2005)

Figure 2. The maize leaf is composed of four distinct tissues (red circles) organized along the proximal-distal (P-D) growth axis. Sheath tissue is the most proximal and the blade tissue is the most distal. Both are separated at the blade-sheath boundary, by the auricle and ligule.

Figure 3. Shoot apical meristem (SAM) development is controlled by various molecular mechanisms. Peripheral zone (PZ), Central zone (CZ), adaxial and abaxial domains are color coded. The genes that regulate the differentiation of different zones share the same color. Leaf primordia at plastochron stages, p0-p2, are shown developing from the SAM (Modified from Machida et al., 2015).

Figure 4. General plant growth regulatory pathway, using CK as an example, from synthesis to biological function for cytokinin in maize. D, Aspartic Acid; P, Phosphate; CK, Cytokinin; ZmHK1, Zea mays Histidine Kinase1 (Modified from Hopkins & Hüner, 2008).

Figure 5. The chemical structure of four representative cytokinins. The N6 position of adenine is indicated and the side chains are highlighted. (A) Kinetin, the first compound isolated that led to the naming of the phytohormone - cytokinin. (B) Isopentenyl adenine (iP) and (C) *trans*-Zeatin, both isoprenoid-type cytokinins, are the most common naturally occurring cytokinins. (D) Benzyladenine (BAP) is an aromatic cytokinin. (Modified from Hopkins & Hüner, 2008).

Figure 6. The cytokinin signal transduction pathway. Cytokinin are transported to the lumen of the ER from the extracellular space. Cytokinin binding induces the dimerization and autophosphorylation of the acceptor histidine kinase. The phosphorelay system begins with the transfer of the phosphoryl group to an aspartic acid residue (D) in the receiver domain, and then to a histidine residue in a separate histidine phosphotransfer protein (HPT). The phosphorylated HPT migrates into the nucleus where the phosphoryl group is transferred a type-B response regulator (RR-B). The activated RR-Bs then activate transcription of cytokinin primary response genes, including the type-A response regulators (RR-As). The RR-As may down-regulate cytokinin responses by suppressing the activation of B-type response regulators.

Figure 7. *Hairy Sheath Frayed1 (Hsf1)* disrupts leaf patterning. On the top is a wild-type leaf blade margin and the bottom is a *Hsf1*/+ mutant leaf blade margin. The prong refers to the abnormal ectopic outgrowth consisting of proximal tissue in

the distal margin of the blade. Close up of prong. Bl, Blade; Au, Auricle; Li, Ligule; Sh, Sheath (Yellow). P, Proximal; D, Distal (Red

Figure 8. An *aberrant phyllotaxy1* (*abph1*) mutant plant showing the paired leaf phyllotaxy phenotype of the *abph1* mutant.

Figure 9. Transcriptome analysis of initiating *Hsf1* prongs. (A) SEM of young leaf primordia from wild type (left) and *Hsf1*/+ (right) plants showing the three margin tissues - wild type (**W**), *Hsf1* no-prong (**N**) and *Hsf1* prong (**P**) (arrows) - captured by laser capture microdissection (LCM) used for transcriptome analysis. (B) Cross section of a *Hsf1*/+ shoot apex showing leaf margins before and after LCM collection of prongs (P) cells. (C) The number of differentially expressed (DE) genes in pair-wise tissue comparisons (p-value < 0.01) out of 20,742 expressed genes.

Figures

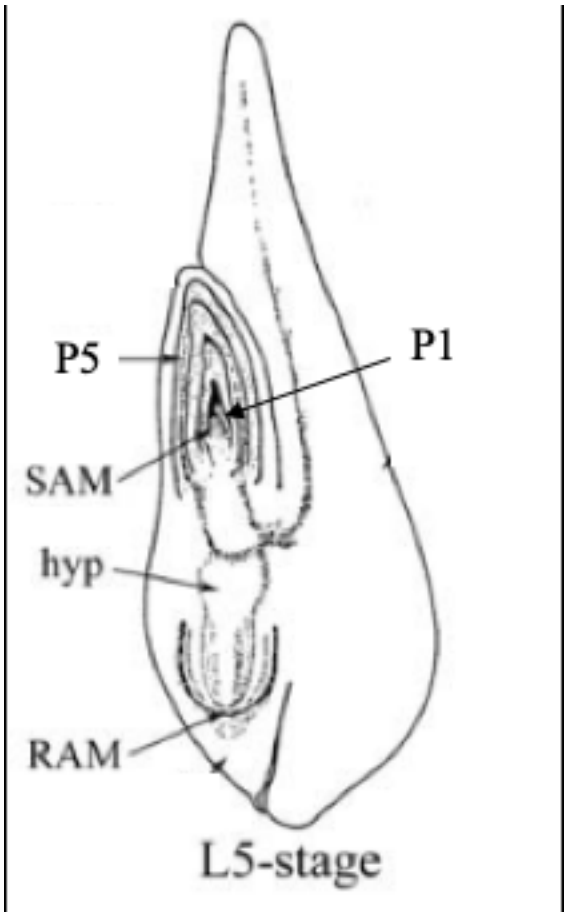

Figure 1. Overview of a maize embryo with five leaf primordia. The outer most leaf is P5, which was the first primordium initiated from the shoot apical meristem (SAM), and will be the first to emerge from the coleoptile. The innermost leaf is the P1. It is the most recently initiated primordium, and is the leaf primordium closest to the SAM (Modified from Zimmermann & Werr, 2005)

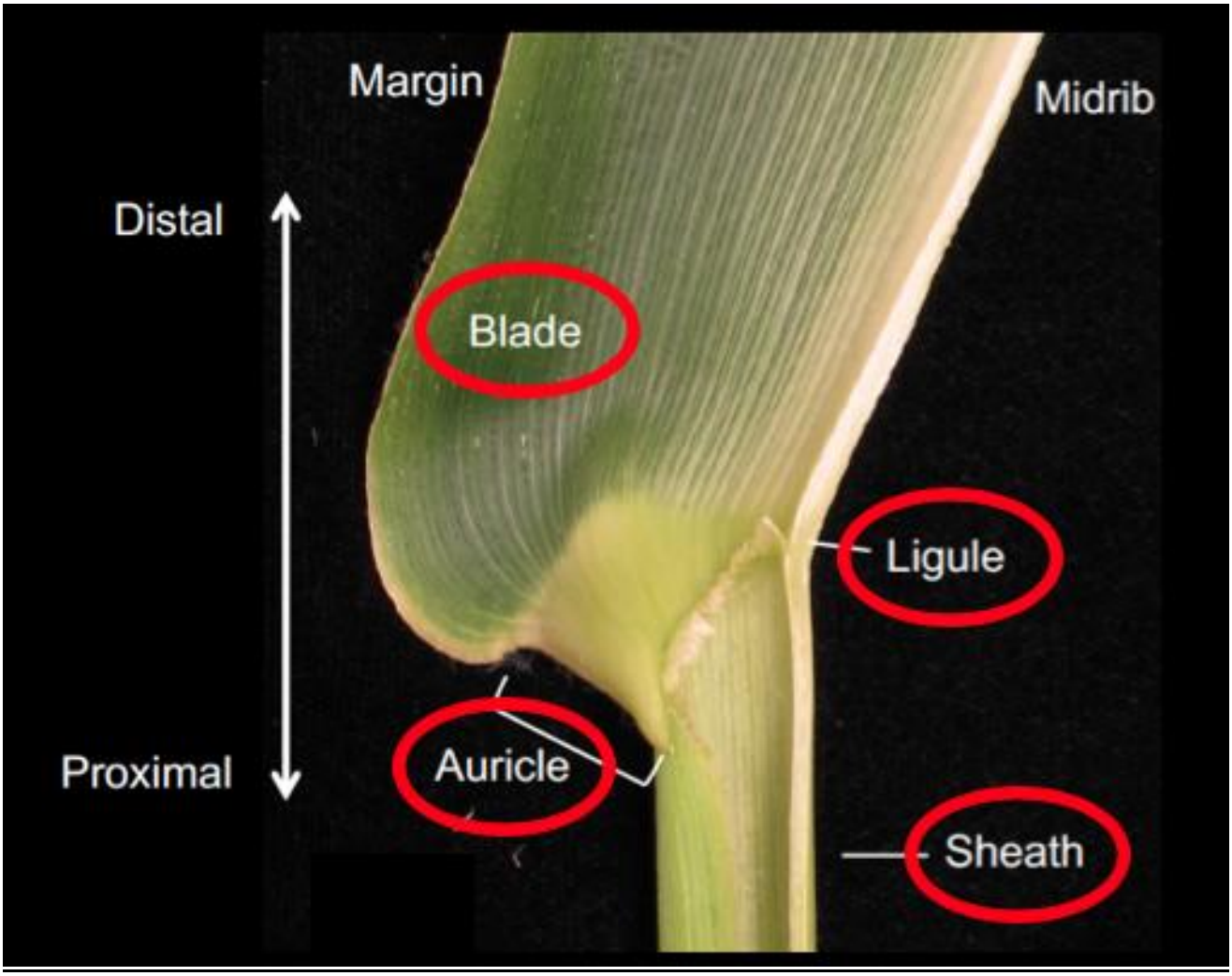

Figure 2. The maize leaf is composed of four distinct tissues (red circles) organized along the proximal-distal (P-D) growth axis. Sheath tissue is the most proximal and the blade tissue is the most distal. Both are separated at the blade-sheath boundary, by the auricle and ligule.

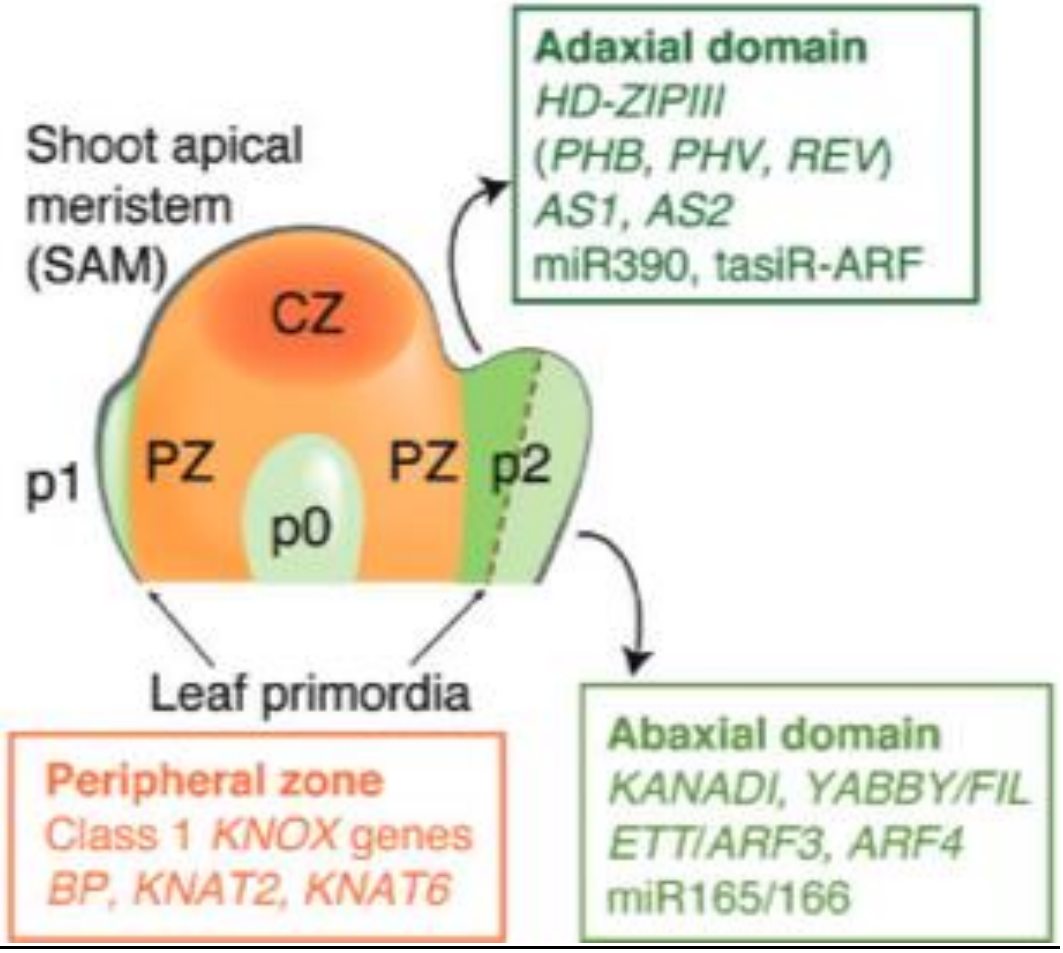

Figure 3. Shoot apical meristem (SAM) development is controlled by various molecular mechanisms. Peripheral zone (PZ), Central zone (CZ), adaxial and abaxial domains are color coded. The genes that regulate the differentiation of different zones share the same color. Leaf primordia at plastochron stages, p0-p2, are shown developing from the SAM (Modified from Machida et al., 2015).

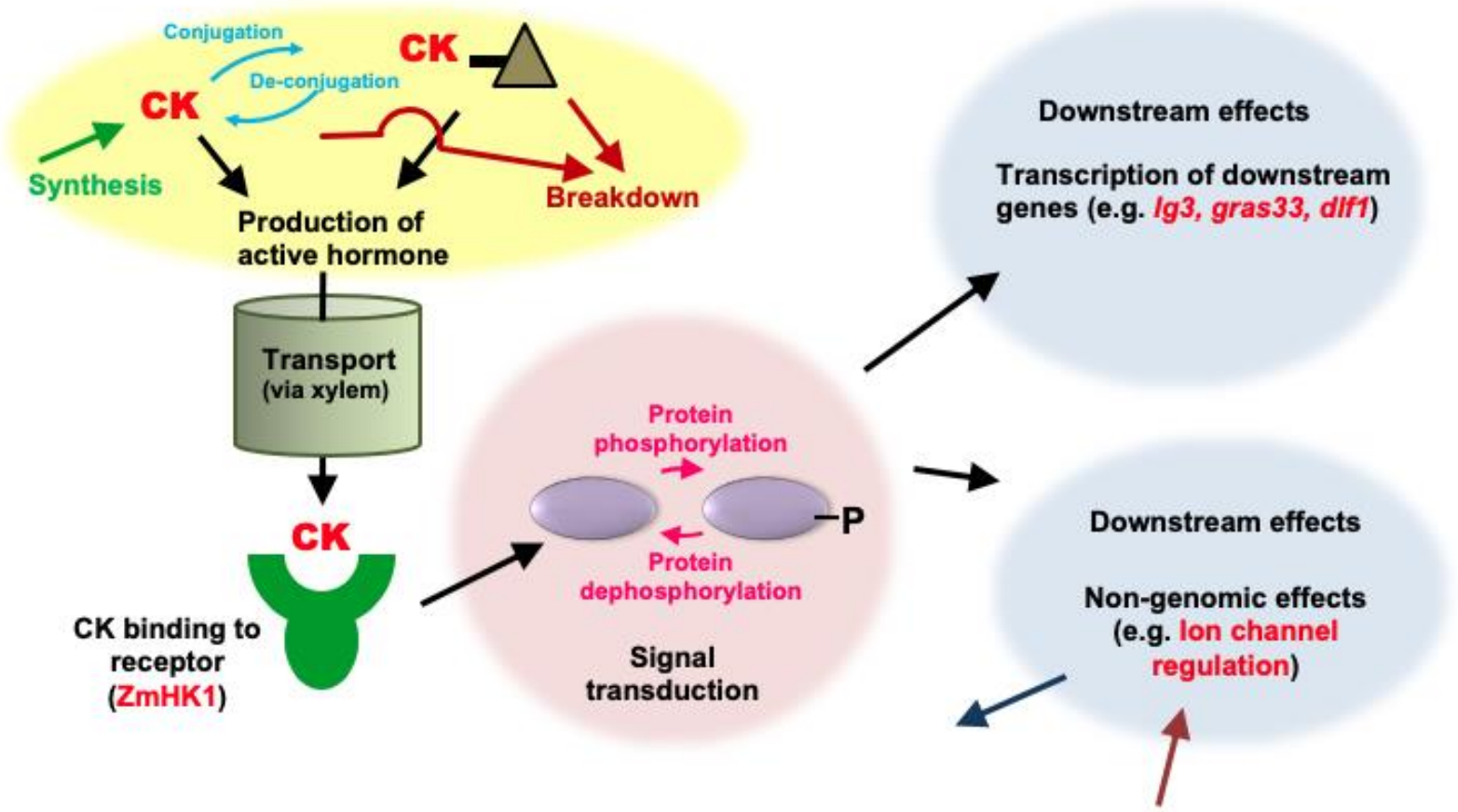

Figure 4. General plant growth regulatory pathway, using CK as an example, from synthesis to biological function for cytokinin in maize. D, Aspartic Acid; P, Phosphate; CK, Cytokinin; ZmHK1, Zea mays Histidine Kinase1 (Modified from Hopkins & Hüner, 2008).

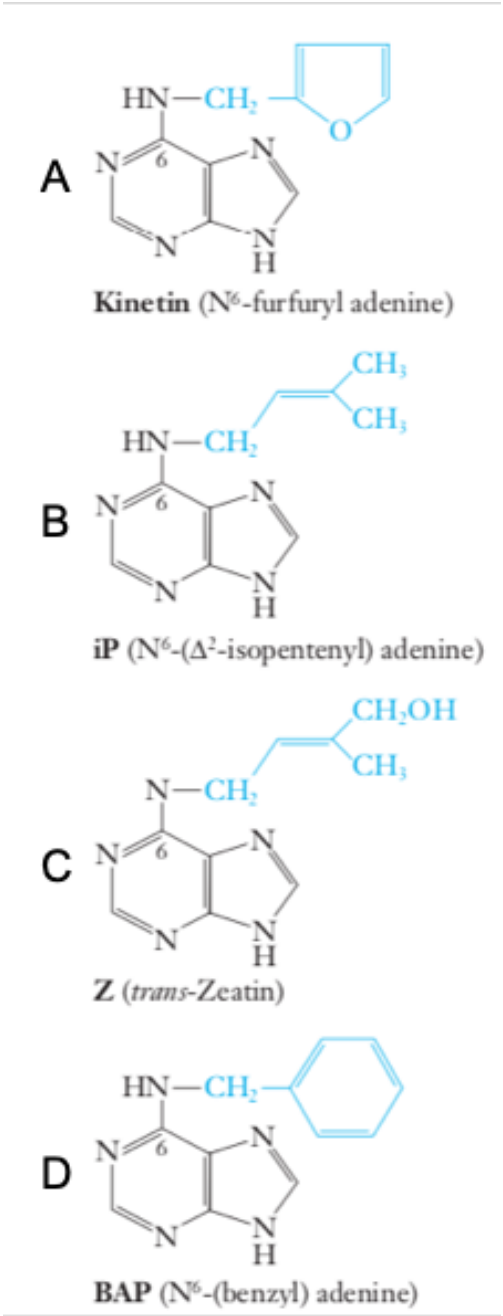

Figure 5. The chemical structure of four representative cytokinins. The N6 position of adenine is indicated and the side chains are highlighted. (A) Kinetin, the first compound isolated that led to the naming of the phytohormone - cytokinin. (B) Isopentenyl adenine (iP) and (C) *trans*-Zeatin, both isoprenoid-type cytokinins, are the most common naturally occurring cytokinins. (D) Benzyladenine (BAP) is an aromatic cytokinin. (Modified from Hopkins & Hüner, 2008).

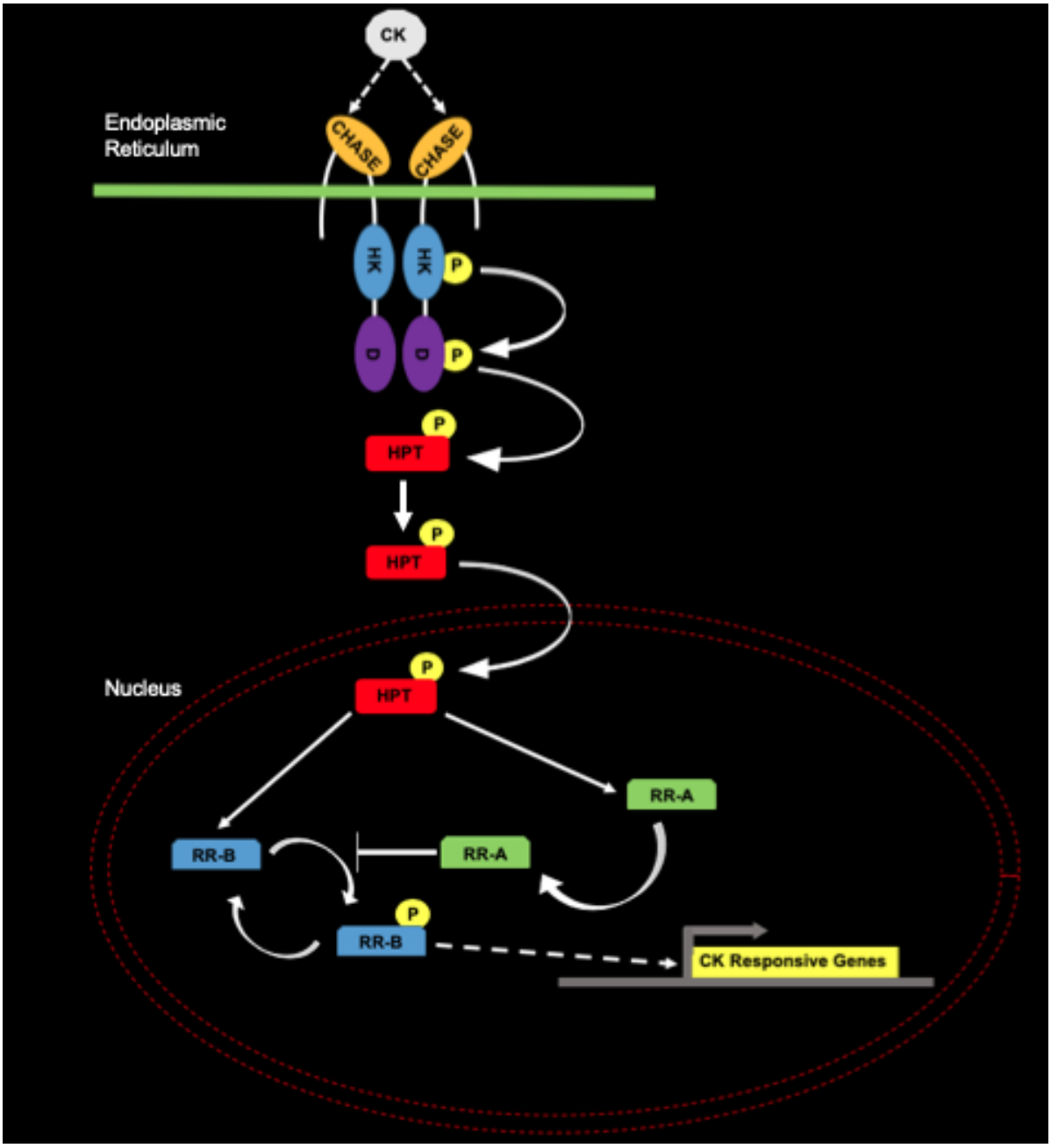

Figure 6. The cytokinin signal transduction pathway. Cytokinins are transported to the lumen of the ER from the extracellular space. Cytokinin binding induces the dimerization and autophosphorylation of the acceptor histidine kinase. The phosphorelay system begins with the transfer of the phosphoryl group to an aspartic acid residue (D) in the receiver domain, and then to a histidine residue in a separate histidine phosphotransfer protein (HPT). The phosphorylated HPT migrates into the nucleus where the phosphoryl group is transferred a type-B response regulator (RR-B). The activated RR-Bs then activate transcription of cytokinin primary response genes, including the type-A response regulators (RR-As). The RR-As may down-regulate cytokinin responses by suppressing the activation of B-type response regulators.

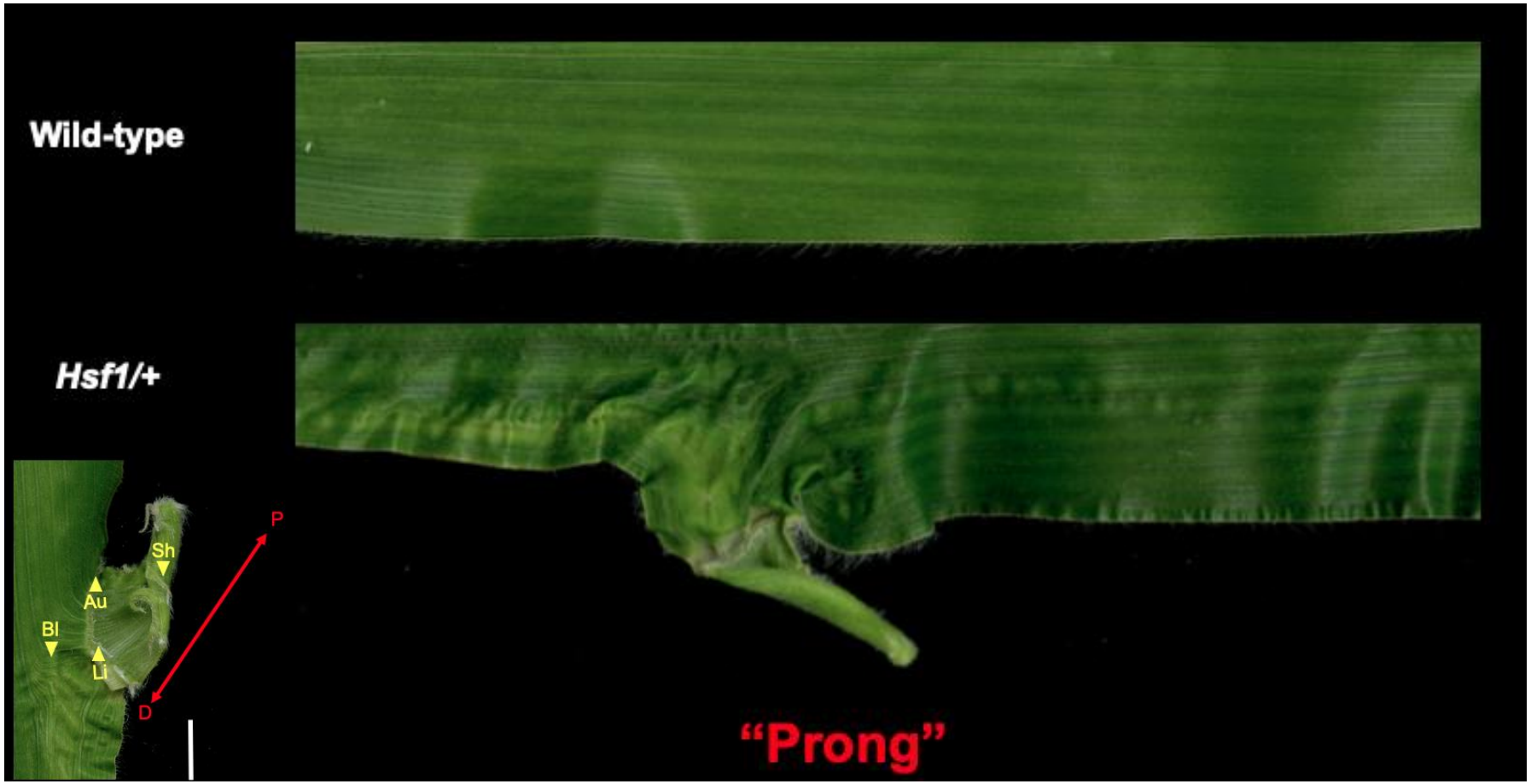

Figure 7. *Hairy Sheath Frayed1 (Hsf1)* disrupts leaf patterning. On the top is a wild-type leaf blade margin and the bottom is a *Hsf1/+* mutant leaf blade margin. The prong refers to the abnormal ectopic outgrowth consisting of proximal tissue in the distal margin of the blade. Close up of prong. Bl, Blade; Au, Auricle; Li, Ligule; Sh, Sheath (Yellow). P, Proximal; D, Distal (Red).

Figure 8. An *aberrant phyllotaxy1* (*abph1*) mutant plant showing the paired leaf phyllotaxy phenotype of the *abph1* mutant.

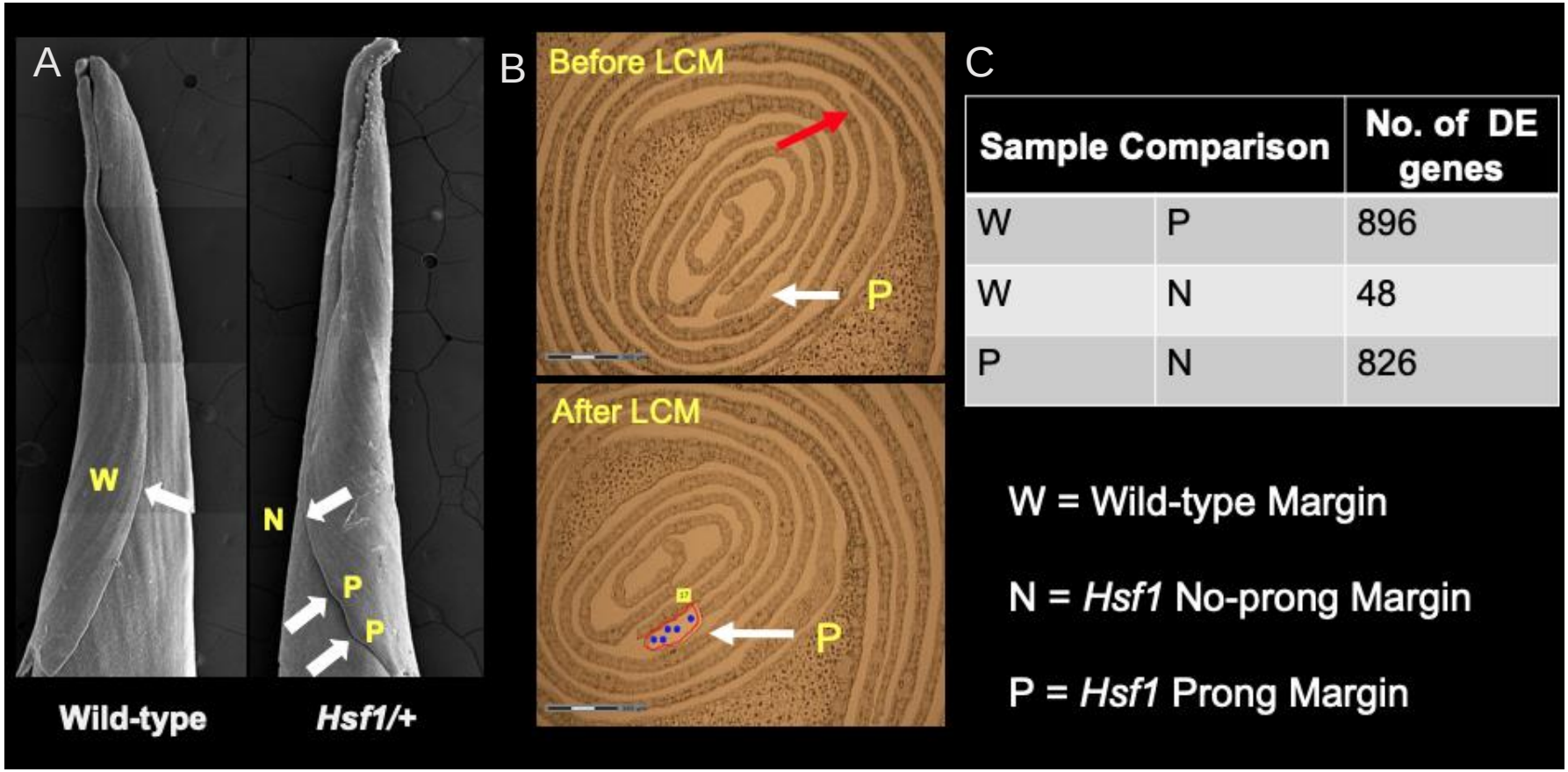

Figure 9. Transcriptome analysis of initiating *Hsf1* prongs. (A) SEM of young leaf primordia from wild type (left) and *Hsf1*/+ (right) plants showing the three margin tissues - wild type (**W**), *Hsf1* no-prong (**N**) and *Hsf1* prong (**P**) (arrows) - captured by laser capture microdissection (LCM) used for transcriptome analysis. (B) Cross section of a *Hsf1*/+ shoot apex showing leaf margins before and after LCM collection of prongs (P) cells. (C) The number of differentially expressed (DE) genes in pair-wise tissue comparisons (p-value < 0.01) out of 20,742 expressed genes.

Tables

Gene Model:	Locus Name:	W:	P:	N:	B73 coordinates (v3):	Functional Group:
GRMZM2G039867	*tru1*	0.2	616.2	8.6	(Chr3:151328862..151332856)	Ankyrin repeat family protein / BTB/POZ domain
GRMZM2G026556	ZmBOPA	0.1	501.3	3.3	(Chr2: 147042526.. 147045597)	
GRMZM2G022606	ZmBOPB	0.0	425.4	0.6	(Chr10:1445596..1448353)	
GRMZM2G060723	*tru-like1 (trl1)*	0.0	239.3	0.4	(Chr8: 158528915.. 158532152)	
GRMZM2G055204	ZmWIND1B	628.8	1420.6	1616.9	(Chr5: 208210507.. 208213447)	APETALA2/ETHYLENE RESPONSIVE FACTOR (AP2/ERF)
GRMZM2G029323	ZmWIND1A	191.9	528.2	391.1	(Chr4: 181088255.. 181090094)	
GRMZM2G071101	ZmWIP2A	0.2	694.2	35.3	(Chr4: 199174315.. 199177504)	Cystein2 Histidine2 (C2H2-type ZF)
GRMZM2G445684	ZmWIP2B	0.9	393.6	3.0	(Chr1: 187302643.. 187305442)	
GRMZM2G079470	GRAS33	399.0	4839.8	513.0	(Chr1: 88488422.. 88491040)	GRAS family
GRMZM2G067921	*dlf1*	181.1	2837.4	329.0	(Chr7: 175583965.. 175585451)	Basic Leucine Zipper Domain (bZIP)
GRMZM2G087741	*lg3*	1.7	3062.9	5.5	(Chr3: 53883227.. 53893066)	KNOTTED1-like homeobox (KNOX)
GRMZM2G328438	*zhd11*	152.8	590.1	178.6	(Chr8: 73654879..73656447)	Zinc Finger-Homeodomain (ZF)-HD
GRMZM2G089619	*zhd15*	59.2	2393.9	210.9	(Chr2: 50140925.. 50142374)	
GRMZM5G821755	*zhd21*	69.4	726.7	83.3	(Chr3: 136934215..136936196)	
GRMZM2G346920	*zhd3*	434.3	2052.5	593.6	(Chr1: 200897499.. 200899336)	
GRMZM2G414844	*zhd6*	21.0	118.2	56.8	(Chr6: 166375940..166377410)	

Table 1. A subset of differentially expressed (DE) transcription factor genes in initiating prongs that were chosen for analysis based on RNA-seq data. W, P, and N are transcript reads per million (RPM). Chromosomal location and functional groups are also listed.

HYPOTHESIS AND OBJECTIVES

Based on previous experiments and unpublished results, I hypothesize that *the genes DE in developing prongs are involved in organ formation and that prongs arise from reprogramming of blade margin cells to take on proximal leaf identity*. To better understand the molecular mechanisms influencing spatial organization of cells in leaf development, I propose three objectives:

1. Determine how expression of key DE genes changes through prong development.
2. Determine the epistatic interaction of mutations of DE genes and *Hsf1.*
3. Characterize a novel genetic enhancer that influences the *Hsf1* phenotype.

OBJECTIVE 1 - EXPRESSION ANALYSIS: PRONG DEVELOPMENTAL STAGES

Introduction

Since the previous RNA-sequencing was conducted on margins sampled at one developmental stage, initiating prongs, one question that remains is: *How does the expression of these DE genes change over time through prong development?* If prongs are essentially new leaf primordia arising from the blade margin, then I expect their development to resemble normal leaf primordia development. In addition, I expect the known regulators of leaf initiation and development to be expressed at the correct developmental stages [Figure 3]. To test this hypothesis, I collected all leaves from *Hsf1/+* mutant plants at different developmental stages and observed each leaf for prongs. I noted the plastochron stage of each leaf, the leaf length, the number of prongs, where on the leaf the prongs were located, the size of each prong, and the general morphological state of each prong. Prongs have not previously been documented at different developmental stages, thus these data help to define stage-specific hallmarks for prong development.

Since I hypothesizes that the development of prongs should follow the same developmental trajectory as normal leaf development, I expected to find similar morphological hallmarks in developing prongs These hallmarks include: (1) development of the three domains of the growth zone (cell division, cell elongation, and cell maturation), (2) formation of four distinct tissues (sheath, auricle, ligule, and blade), and (3) polarization of these four tissues along a growth axis. In general, early stage immature leaf primordia do not contain the four distinct tissues and are mostly consist of

nondifferentiated cells that are dividing and elongating. However, the first indication that the developing leaf establishes proximal and distal identities occurs when a distinct, uniquely linear band of smaller cells forms which runs perpendicular to the proximal-distal axis of the developing leaf. This line of cells is called the pre-ligule band (PLB) and forms by localized anticlinal divisions, with new cell walls forming perpendicular to the existing cell walls, in the adaxial epidermis. The PLB begins to develop at the midrib of the leaf, and gradually grows towards each margin. The formation of the PLB is the first sign of proximal-distal polarity of the leaf by initiating a blade-sheath boundary [Figure 10]. Once the PLB is established the cells that are to become the blade and sheath tissue are determined.

A close inspection of developing prongs in *Hsf1* plants revealed key morphological differences that resemble normal leaf development. I used these hallmarks to define three stages of prong development: emerging, transitioning, and maturing. There is an unknown molecular mechanism that dedifferentiates the margin tissue back into meristematic tissue seemingly reinitiating the formation of new leaves, which result in the phenomenon referred to here as “Prongs” (Bertrand-Garcia & Freeling, 1991).

Once these stages were defined, I collected developing prongs at each of these three stages for expression analysis. In addition, normal appearing blade margin tissue (=no-prong) was collected from *Hsf1* plants as developing prongs were collected, and wild type tissue was collected from blade margins of similar stage. Gene specific primers were developed for the DE gene set in Table 1and used to perform RT-qPCR to measure the expression levels for each of the DE genes through prong developmental.

Materials and Methods

Genetic Stocks

Hsf1-1603 is the allele used in this research and if referred to as *Hsf1* throughout this thesis. *Hsf1-1603* was produced by EMS mutagenesis treatment of the inbred line Mo17. *Hsf1-1603* was backcrossed to B73 more than ten generations and this is the material used in my thesis research unless otherwise noted. Because homozygotes of *Hsf1* are lethal, all the analyses were performed using the heterozygote class.

Growth Conditions

Seeds were treated with Baytan® T to prevent mold and fungal growth and planted in 32-well growing flats in the William T. Pope Greenhouse at the University of Hawai'i- Mānoa (Honolulu, HI). Seedlings were transplanted into 3-gallon pots once the fifth seedling emerged and leaf four was fully collared. The fifth leaf was marked to track leaf number as the plants matured.

Dissection Methods

Ten *Hsf1/+* seeds were planted in three biological replicates and dissected at growth stages v10 (Hanway, 1966). A head mounted magnifying glass was used to identify prong tissue on *Hsf1/+* leaves for each replicate. When a prong was identified, the developmental stage and location on the margin was determined and recorded. Using fine point tweezers and a razor blade, tissue was collected and placed in either formaldehyde-acetic acid alcohol (FAA) for histology or TRizol (Life Technologies) for RNA isolation.

Key hallmarks separate prong developmental stages

To distinguished prongs at emerging, transitioning and maturing developmental stages, a 3D phone image adapter schematic was created and printed through the University of Hawai'i's Innovation Lab [Figure 11]. This allowed for rapid collection of images of developing prongs (on average 35 images/hour) using a cell phone. Histological analyses of prong tissue revealed hallmarks that distinguished prongs at the three developmental stages.

Fixation of Tissue for Histological Purposes

Tissue were collected using fine point tweezers and a sterilized razor blade, then placed in fixative solution. Tissue were fixed in FAA (75% ethanol, distilled H_2O, 10% formaldehyde solution, and 5% glacial acetic acid) in1.5 mL centrifuge tubes and stored at 4^{o} C.

Fixed leaf samples were mounted on a glass slide using the floating sample technique (Aimee Naomi Uyehara, 2018). Briefly, tissue was gently placed in a container of distilled water, at which point the fixed leaf sample would float, allowing for the easy transfer to a glass slide. A glass cover slip was then placed on top, making sure the tissue would lay flat. Once the margin samples were mounted on individual slides, images were taken of the abaxial and adaxial sides.

Expression Primer Design

Gene specific primer were designed for each DE gene [Table 2], using its complementary DNA (cDNA) sequence from MaizeGDB, version 3, (v.3, Portwood et al., 2018) and cDNA sequence from Gramene (B73_RefGen_v4) (Tello-Ruiz et al., 2018). Primers were designed using Primer3 (v. 0.4.0, Untergasser et al., 2012)

following standard design parameters. Each pair of primers was tested, and PCR conditions were optimized using cDNA synthesized from two independent B73 shoot apices and gradient PCR.

RNA Isolation and cDNA Synthesis

RNA was isolated from the five tissue types (emerging prong (E), transitioning prong (T), mature prong (M), no-prong (N), and wild type (W)) for three reps for a total number of five hundred and forty samples using TRIzol (Life Technologies) protocol according to the manufacturer's recommendations. RNA concentrations were measured using a NanoDrop ND1000 spectrophotometer.

For cDNA synthesis, qScript cDNA SuperMix (Quanta Biosciences) was used following manufacturer's recommendations. The amount of total RNA used for each cDNA synthesis was determined using the lowest concentration of RNA obtained from that day's extractions to equal 10 ng/µl total RNA for the template.

RT-PCR and qPCR Methods

PCR reactions using iQ™ SYBR® GREEN (BIO-RAD) were carried out in 96-well Hard-Shell®PCR Plates (BIO-RAD). For each sample, a 10 µl master mixture was made by combining 4 µL cDNA with 1X iQ™ SYBR® GREEN Supermix (BIO-RAD) and gene-specific primers to a final concentration of 300 nM each. The 10 ul reactions were aliquoted into the 96-well plates which were sealed with ThermalSeal RT2RR™ Sealing Films (EXCEL Scientific, Inc.). PCR was run in the CFX96™ Real-Time System C1000 Touch Thermal Cycler using the following amplification parameters: 3 min at 95°C initial denaturation followed by 10 s at 95°C, 1 min at 58°C repeating for 39 cycles and 5 s at

65°C, ending with 50 s at 95°C. Post-run data QC and analysis were performed according to the manufacturer's instructions and as described below.

The relative expression of each gene was calculated using $-2^{(\triangle\triangle Cq)}$ (Schmittgen & Livak, 2008). The internal control gene was FPGS which encodes a folylpolyglutamate synthase (Manoli, Sturaro, Trevisan, Quaggiotti, & Nonis, 2012) and was determined to be a reliable internal housekeeping control gene with stable expression in many different maize tissues and developmental stages. An ANOVA test and a Tukey's HSD were run on the relative expression for each gene. Multicomparison test was set at a confidence of 95% ($p<0.05$) to compare each tissue type for the genes of interest. P-values that were <0.05 were considered statistically significant and therefore different, while values ≥ 0.05 were not.

Results

Key hallmarks define prong developmental stages

I determined that there were three specific stages of a developing prong: (1) emerging, (2) transitioning, and (3) maturing, based on my morphological observations. The earliest indication of prong development was the enation (“bump”) of tissue growing from the blade margin. This was also marked by the bending of the normally parallel vasculature tissue towards the margin outgrowth [Figure 12A]. Prongs in this category were defined as emerging (E). The second category of developing prongs was defined by the presence of the PLB. Consistent with normal leaf development, the PLB marks the beginning of P-D polarity and will eventually differentiate into a ligule. Prongs having a noticeable PLB were defined as transitioning (T), since they were at a middle stage of development. The last category of prongs was defined by the resemblance of the prong to a photosynthetically competent leaf. Prongs in this category were called mature (M) and were green, had fully developed bulliform cells (bubble-shaped epidermal cells) that give rise to prominent macrohairs at the prong margin. The mature prongs also had a more fully developed sheath, ligule and auricle [Figure 12B&C].

Along with collecting tissue for histological and RNA purposes, I also recorded what leaf and the location on the leaf the prong samples were taken. Using total leaf length and dividing the leaf into quadrants, I determined that on average most prongs (> 60%) developed in the basal 25% of the blade and gradually prong formation decreased closer to the distal portion of the leaf [Figure 13]. Further analysis of the prong stage and location determined that all three stages collected (E, T, and M) were found to be more abundant in the most proximal regions of the leaf [Table 3]. Since almost all

prongs formed in the basal 50% of the blade, it is not surprising all prong stages were represented in that part of the leaf [Table 3].

Expression of DE genes through prong development

Gene-specific primers were developed for each of the seventeen DE genes. Each of these primer sets were tested individually on cDNA isolated from the shoot apex of two independent B73 inbred plants before performing qPCR. PCR products were run on gel electrophoresis and amplification of a single band of expected size confirmed the primers were specific [Table 2]. If PCR amplified products of unexpected size or multiple products, the amplification products were subcloned into the pGEM®-T Easy Vector Systems (Promega) and then transformed into *E. coli*. Plasmids containing inserts were isolated via the Alkaline Lysis Method (bio-protocol) and sent for sequencing to GENE-WIZ center ("Genewiz - Solid Science. Superior Service.," N.D.). The sequencing results allowed construction of an improved consensus sequence from which I designed more specific gene primers.

Previous RNA-sequencing produced expression values for one developmental stage. To determine the expression of DE genes from initiating to mature prongs, IQuantitative PCR was used. Utilizing the FPGS gene as the internal control, expressed in all the tissue types, the qPCR analysis revealed that ten out of the seventeen genes of interest were expressed at detectable levels in all/most of the samples. These included, *delayed flowereing1* (*dlf1*) [Figure 14], *gras33* [Figure 15], *liguleless3* (*lg3*) [Figure 16], WIND1A and WIND1B [Figure 17], WIP2B [Figure 18], and the 4 BOP family genes [Figure 19]. To confirm the expression results, each qPCR amplification product was run on 2% gel electrophoresis to see if the relative amount of product

seemed to match the reported C_q values. The C_q values ranged from 0 to 40 indicating some qPCR reactions produced no products while others were likely producing artefacts. qPCR of some DE genes had C_q values of 35 to 40 but did not produce an amplification product. These high values and no amplification samples were considered as failed reactions and therefore the C_q value was set to 0. Even though the primers were tested for each target and proved to be specific enough, there were seven samples out of the seventeen that gave unreliable results. Therefore, this variation led to the elimination of these samples from further analysis.

For the ten samples that showed reliable results, expression differences between the five types of tissue – E, T, M, N and W - were determined by ANOVA and a Tukey's HSD for each gene. A Tukey's HSD confidence of 95% ($p \leq 0.05$) was used to determine that there was a significant difference in DE gene expression among the five tissues.

The *delayed flowering1* (*dlf1*) gene encodes a basic-leucine zipper (bZIP) TF that promotes the floral transition by interacting with the mobile floral signal ZCN in the shoot apex (Muszynski et al., 2006). The loss-of-function *dlf1* mutant, shows a prolonged vegetative growth state, resulting in later flowering (ca. 2 weeks), and taller plants with more leaves. The *dlf1* gene is expressed in the SAM and emerging leaf primordia but has not been shown to have any influence on organ formation (Muszynski et al., 2006). For *dlf1*, expression was high in emerging prongs and increased in transitioning prongs before dropping to low levels in mature prongs, similar to wild type. These relative expression trends compliment the RNA-seq data (W: 181 RPM, P: 2837 RPM, N: 329 RPM). Surprisingly, expression in no-prong was as high as emerging prongs. This is possibly different from the initial RNA-Seq result and may indicate my no-prong margin

tissue was somehow developmentally different from the no-prong tissue collected for RNA-Seq analysis. Alternately, the RNA-Seq or my qPCR results might be wrong. Expression analysis with *dlf1* should be repeated.

The GRAS family of TFs encodes VHIID regulatory proteins that play diverse roles in plant development (Bolle, 2004). The maize GRAS33 gene identified in the RNA-Seq data is highly homologous to the tomato *Lateral Suppressor* (*Ls*) GRAS TF that controls axillary meristem growth (Ls ref). The *GRAS33* gene expression was not as expected based on the RNA-seq data (W: 399 RPM, P: 4839 RPM, N: 513 RPM). My results indicated *GRAS33* was expressed the same across the E, M, N and W tissues and higher in T. Given a presumed role in organogenesis for *GRAS33*, I expected its expression to drop in T and M and be lower in both N and W, relative to E. This gene may play a different role in prong formation or my expression results need to be repeated.

The *lg3* gene encodes a class I KNOX TF and class I KNOX proteins have been shown to play critical roles in meristem maintenance within all higher plant species (KNOX refs here). Loss-of-function *lg3* mutations did not show any obvious developmental phenotypes likely owing to redundancy for *KNOX* genes that are expressed in the shoot apex in maize (Bauer et al., 2004) I expected *lg3* expression to mark tissue that has some meristematic activity. As expected, expression of the *lg3* gene was higher in E and T prongs, presumably because these stages retain some meristematic activity. This expression pattern is consistent with the RNA-Seq expression (put RPMs here) which shows high expression in initiating prongs and no expression in N and W margins which have already differentiated,

The *WOUND INDUCED DEDIFFERENTIATION 1* (*WIND1*) gene encodes an *AP2/ERF* transcription factor that is a key regulator of dedifferentiation (Ikeda & Ohme-Takagi, 2014; Iwase, Mitsuda, et al., 2011; Iwase, Ohme-Takagi, & Sugimoto, 2011). Expression of this gene occurs with plant wounding and is required for differentiated plant cells to dedifferentiate and assume new cellular identities. Two duplicate *WIND1* homologous genes were present in the DE gene set, *ZmWIND1A* and *ZmWIND1B*. I expect expression of both these genes to occur in tissue that is dedifferentiating. For the *ZmWIND1A* and *ZmWIND1* B genes, that had an RPM expressed higher in the prong margin tissue and no-prong margin in the RNA-seq data, provided unexpected results for the relative expression. Expression of *ZmWIND1A* was different in the wild-type margin compared to the other developmental stages, while *ZmWIND1B* did not show any difference in any tissue types.

ZmWIP2B is a member of the family of C_2H_2 zinc-finger proteins (ZFPs) are considered to be one of the largest transcription factor class regulatory families in plants (Englbrecht, Schoof, & Böhm, 2004; Iuchi, 2001). C_2H_2 type of zinc-finger TFs are known to play a in abiotic stresses and hormone signal transduction (Muthamilarasan et al., 2014). I expected the *ZmWIP2B* expression to be higher in the developing prongs due to the hypersignaling of CK in the *Hsf1/+* mutants. Results from the qPCR results showed that *ZmWIP2B* had significantly higher relative expression in the three prong stages compared to the wild-type and no-prong tissues, as expected.

Maize genes homologous to *BLADE-ON-PETIOLE1* (*BOP1*) in *Arabidopsis,* and other BOP-family genes have been identified in the prong RNA-seq dataset to be DE. *BOP1* encodes a BTB/POZ protein that is known to repress class I *KNOX* genes during

leaf initiation (Dong et al., 2017). Most recently the *BOP* genes have been shown to influence blade to sheath ratio and sheath specification in rice (Toriba et al., 2019b), therefore I would expect the BOP genes to be expressed in the early stages of prongs when the sheath identity is being determined. qPCR revealed that the relative expression of all the BOP genes was significantly higher in the emerging and transitioning prong stages when compared to the mature, no-prong, and wild-type tissues.

Discussion

Results from objective 2 provided two major contributions; (1) the first full characterization of hallmarks that distinguish prong developmental stages and (2) determine the expression of the genes of interest over prong development. Prior to this study, prong development had not been comprehensively described. Since we think prongs develop similar to normal leaf development, understanding the cellular changes for prongs as they mature can reveal the molecular networks that regulate leaf development and therefore providing insight into the function of regulatory factors of organogenesis in maize.

I classified prongs into three developmental stages; (1) emerging, (2) transitioning, and (3) maturing. It was determined that for emerging prongs, margin tissue starts to grow perpendicular to the P-D growth axis that is parallel with the midrib. Observing cross sections of the whorl of leaf primordia in the mutant plant shows margins that will develop prongs can be seen as obtuse compared to wild-type and no-prong margins. For transitioning prongs, an alternate P-D polarization is established perpendicular to the leaf when the PLB becomes visible and, therefore, demarcates a new blade to sheath boundary for each prong. One of the striking *Hsf1* mutant phenotypes is the increase in macrohair density. These arise from bulliform cells can be seen at the margin of each maturing prong. Maturing prongs are in the last developmental stage, and, like mature leaves, cells and tissue are fully differentiated. Mature prongs are marked by the presence of sheath, auricle and ligule tissue abutting the blade and the presence of bulliform cells that have formed at a higher density below the macrohairs. For small prongs that lack clear sheath, auricle and ligule tissues, these mature prongs

consist mainly of a cluster of macrohairs atop bulliform cells and give the prong a “caterpillar or eyelash” characteristic. [Figure 12A&B].

Most of the relative expression data showed expected patterns as compared to the RNA-seq data. However, for the genes that did not meet expectations based on RNA-Seq data may be due to the fact that the primer oligos are not specific enough for the intended target, even though they were designed from B73 inbred cDNA sequence and gave positive results when tested against control cDNA. It can also be hypothesized that the genes that gave relative expression opposite than expected could be due to the developmental stage the RNA-seq was collected, since the developmental stages determined in this thesis are not the same as that used for LCM and RNA-seq. Thus, it is possible that the genes that showed differential expression were on at an earlier stage of prong development. Since the LCM was able to capture the tissue at a leaf primordium state the prongs would be initiating, meaning that these genes could be expressed before and turned off by the emerging and later developmental stage. However, the genes that agree with our expectations suggest that they are required for prong development and can influence leaf patterning.

The relative expression of *lg3* met expectations, which was to observe decreasing expression as the prong matures. This would be expected since we predict that prong margin tissue attains some meristematic activity in order to produce a prong. But would lose meristematic activity as the prong differentiates and matures. This is consistent with what is known for the function of class I KNOX genes like *lg3*.

The BOP genes follow identical relative expression with higher expression within the early prong stages, while remaining off in the no-prong and wild-type margins. This

suggests that when the blade to sheath boundary is being determined in the developing prongs these genes are active, supporting the hypothesized meristematic function.

However, the WINDs did not seem to follow a trend and produced unexpected results. WIND1A produced relative expression higher in the wild-type tissue compared the mutant, which is opposite of the RNA-seq data, while the WIND1B does not have any statistical differences between each developmental stage. The unexpected results may be due to these genes being expressed at earlier stages than the developmental stages sampled.

The *dlf1* gene was only previously known to play a role in floral transition in plants, but the relative expression results reveal a possible new function in leaf development. Since relative expression of *dlf1* from the qPCR complimented the RNA-seq data previously produced and it was seen that *dlf1* was expressed significantly higher in the transitioning prongs suggest that this bZIP TF influences the formation of prongs and leaf development.

The GRAS33 gene revealed an unexpected higher relative expression in the transitioning prongs than any other stage or sample type. This suggests an unknown role in prong development and leaf patterning. Further analysis or repeat of the previous studies need to be conducted.

Future Directions

To validate the hypothesis, *DE genes with relative expression patterns that agrees with the RNA-seq data and a presumed function in organogenesis are required for prong development and influence leaf patterning*, double mutant analysis should be conducted. This would require that mutants be made of each DE gene using transgenics or mutagenesis. Then *Hsf1*/+ will need to be crossed to each mutant to produce families segregating wild types, single mutants, and the double mutants. Using the leaf analyses conducted in Objective 2 the double mutants will be compared to *Hsf1*/+ single mutants.

Figure Legends

Figure 10. Scanning electron micrograph (SEM) of the adaxial side of a developing leaf primordia. The lighter cells that make a mound and is denoted by the yellow arrow is the pre-ligule band forming perpendicular to the margins. PLB, pre-ligule band.

Figure 11. 3D printed phone adapter for the dissecting microscope. Picture shows an example of taking images of each prong using a phone camera. Phone holder allowed for consistency between placement and distance for each image.

Figure 12. Prong developmental stages, (A) emerging, (B) transitioning, (C) mature prong. Key characteristic for a transitioning prong is the formation of the pre-ligule band (PLB) (left of the red dotted line), and for mature prongs are increased macrohair density (red triangles) at the margin of the prong.

Figure 13. Prong distribution on a *Hsf1*/+ leaf. Red dotted lines divide the leaf into four quadrants are labeled A-D in a P-D axis. Each is a quarter of the leaf length total. Percentages are the number of prongs in each quadrant/total prong number X 100 and are listed below each quadrant. Red arrow shows the direction of the proximal-distal axis. P Proximal; D Distal.

Figure 14. Relative expression data for *delayed flowering1* (*dlf1*) over developmental stages of the prong. Y-axis, relative expression; X-axis, developmental stages. E, emerging; T, transitioning; M, mature; N, no-prong; W, wild-type. Statistical significance was based on a multicomparison of the means, $P \leq 0.05$.

Figure 15. Relative expression data for *GRAS33* over developmental stages of the prong. Y-axis, relative expression; X-axis, developmental stages. E, emerging; T, transitioning; M, mature; N, no-prong; W, wild-type. Statistical significance was based on a multicomparison of the means, $P \leq 0.05$.

Figure 16. Relative expression data for *liguleless3* (*lg3*) over developmental stages of the prong. Y-axis, relative expression; X-axis, developmental stages. E, emerging; T, transitioning; M, mature; N, no-prong; W, wild-type. Statistical significance was based on a multicomparison of the means, $P \leq 0.05$.

Figure 17. Relative expression data for the maize *WOUND INDUCED DEDIFFERENTIATION* (*WIND*) genes over developmental stages of the prong. (A) *ZmWIND1A* and (B) *ZmWIND1B*), Y-axis, relative expression; X-axis, developmental stages. E, emerging; T, transitioning; M, mature; N, no-prong; W, wild-type. Statistical significance was based on a multicomparison of the means, $P \leq 0.05$.

Figure 18. Relative expression data for maize *TRYPTOPHAN-ISOLEUCINE-PROLINE* (*WIP*) gene over developmental stages of the prong. (*ZmWIP2B*. Y-axis, relative expression; X-axis, developmental stages. E, emerging; T, transitioning; M, mature; N, no-prong; W, wild-type. Statistical significance was based on a multicomparison of the means, $P \leq 0.05$.

Figure 19. Relative expression data for the maize *BLADE-ON-PETIOLE* (*BOP*) genes over developmental stages of the prong. (Top-left) *tassel replaces upper ear1* (*tru1*), (Top-right) *tassel replaces upper ear- like1* (*trl1*), (Bottom-left) *ZmBOPA*, and (Bottom-right) *ZmBOPB*. Y-axis, relative expression; X-axis, developmental stages. E, emerging; T, transitioning; M, mature; N, no-prong; W, wild-type. Statistical significance was based on a multicomparison of the means, $P \leq 0.05$.

Figures

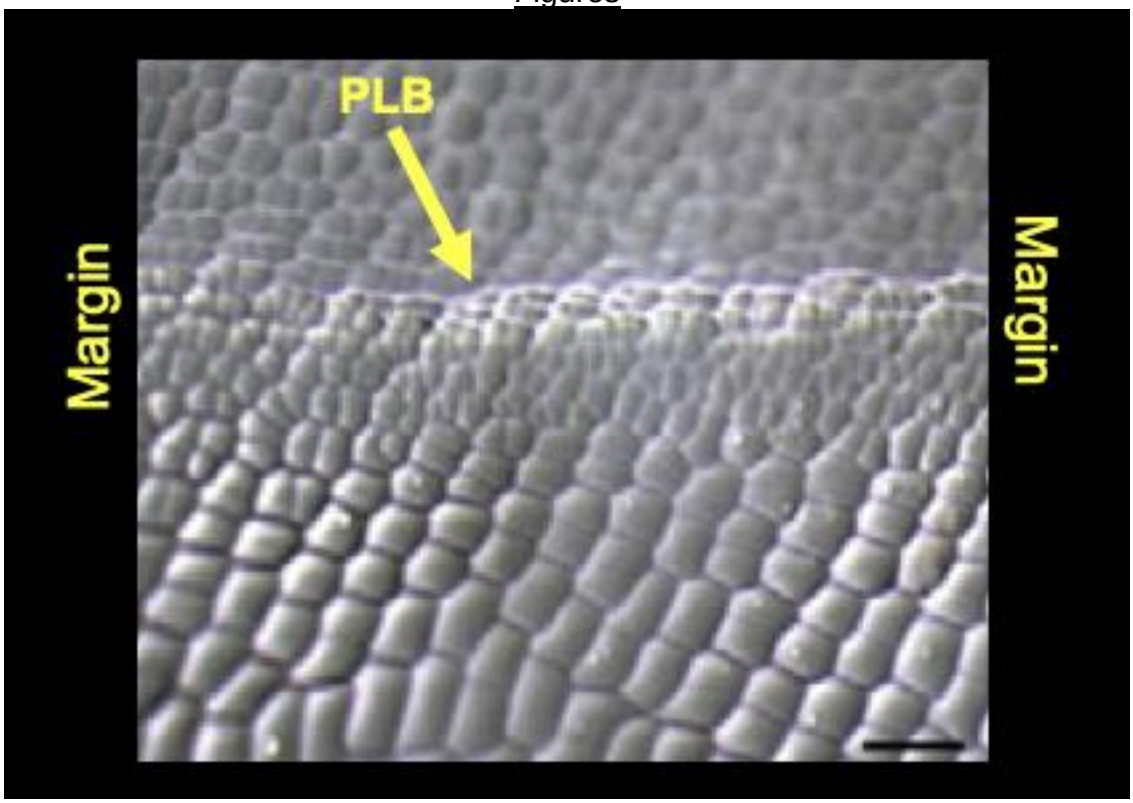

Figure 10. Scanning electron micrograph (SEM) of the adaxial side of a developing leaf primordia. The lighter cells that make a mound and is denoted by the yellow arrow is the pre-ligule band forming perpendicular to the margins. PLB, pre-ligule band.

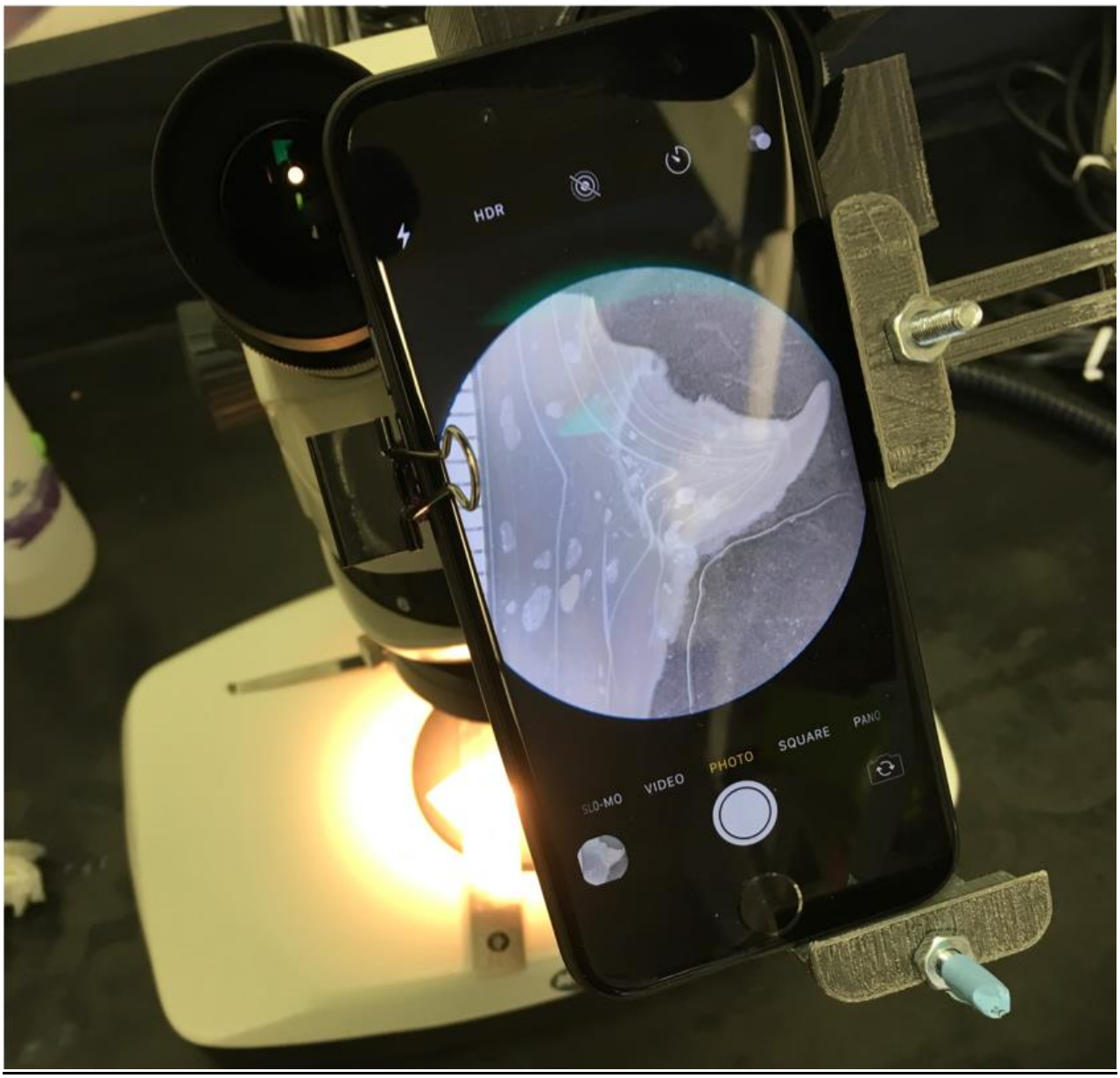

Figure 11. 3D printed phone adapter for the dissecting microscope. Picture shows an example of taking images of each prong using a phone camera. Phone holder allowed for consistency between placement and distance for each image.

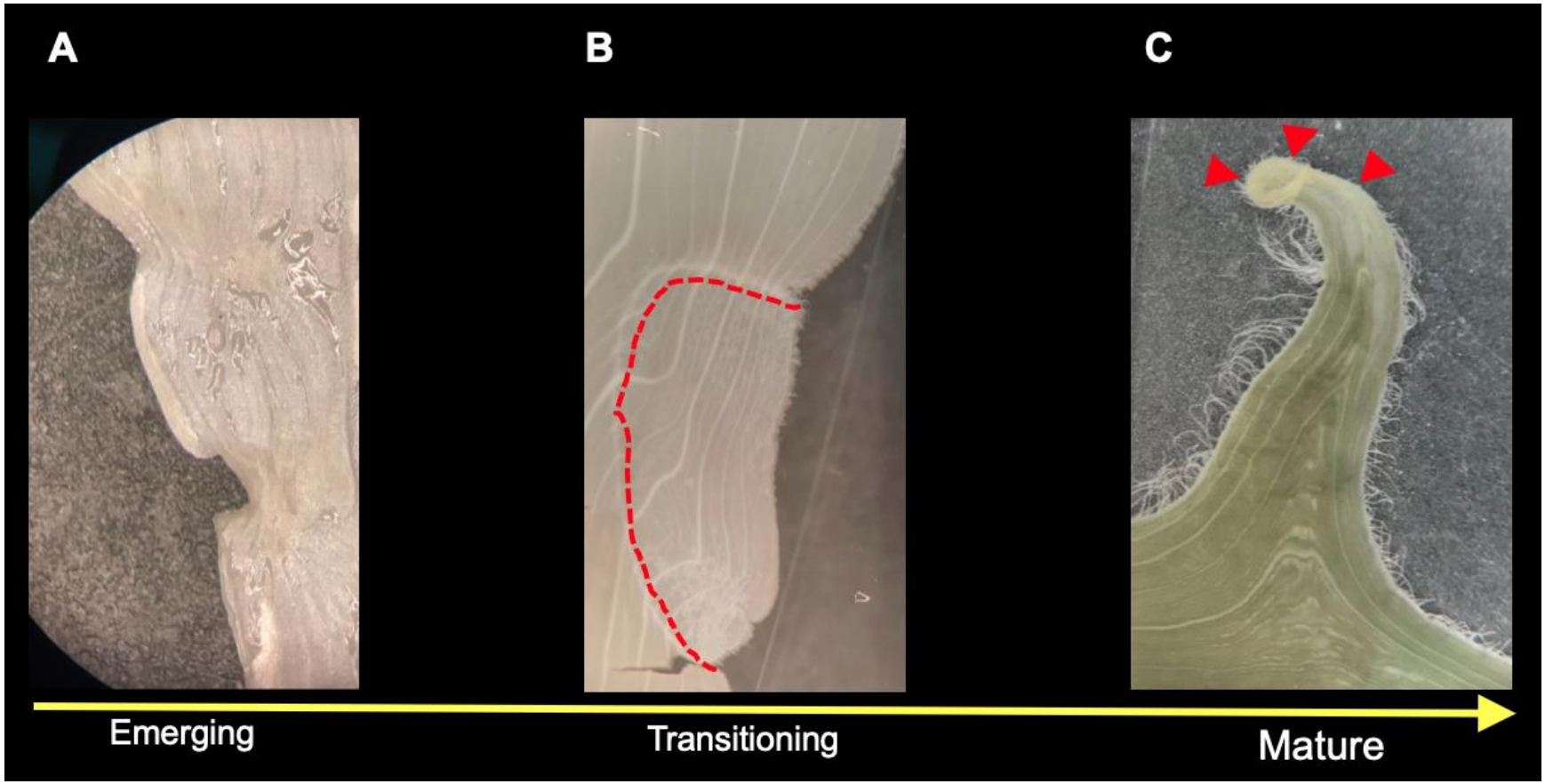

Figure 12. Prong developmental stages, (A) emerging, (B) transitioning, (C) mature prong. Key characteristic for a transitioning prong is the formation of the pre-ligule band (PLB) (left of the red dotted line), and for mature prongs are increased macrohair density (red triangles) at the margin of the prong.

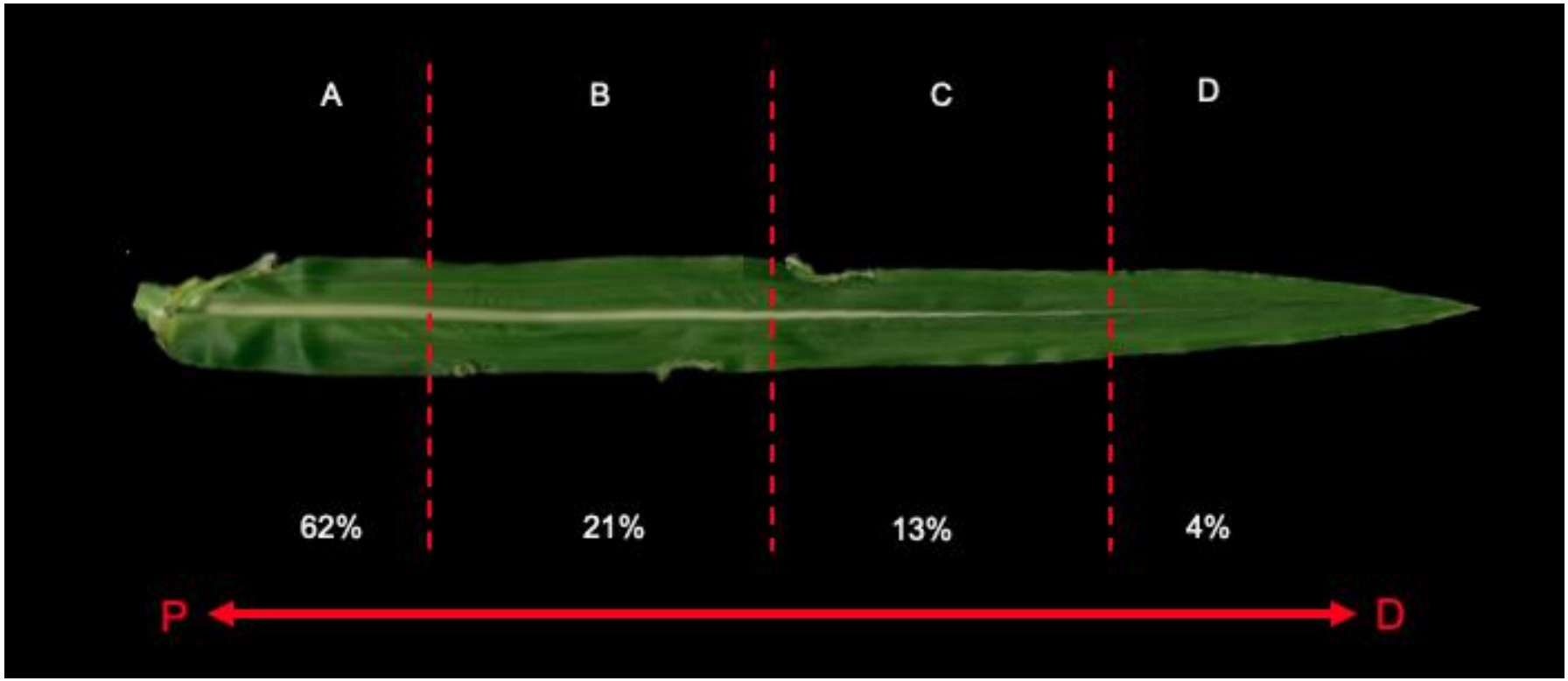

Figure 13. Prong distribution on a *Hsf1/+* leaf. Red dotted lines divide the leaf into four quadrants are labeled A-D in a P-D axis. Each is a quarter of the leaf length total. Percentages are the number of prongs in each quadrant/total prong number X 100 and are listed below each quadrant. Red arrow shows the direction of the proximal-distal axis. P Proximal; D Distal.

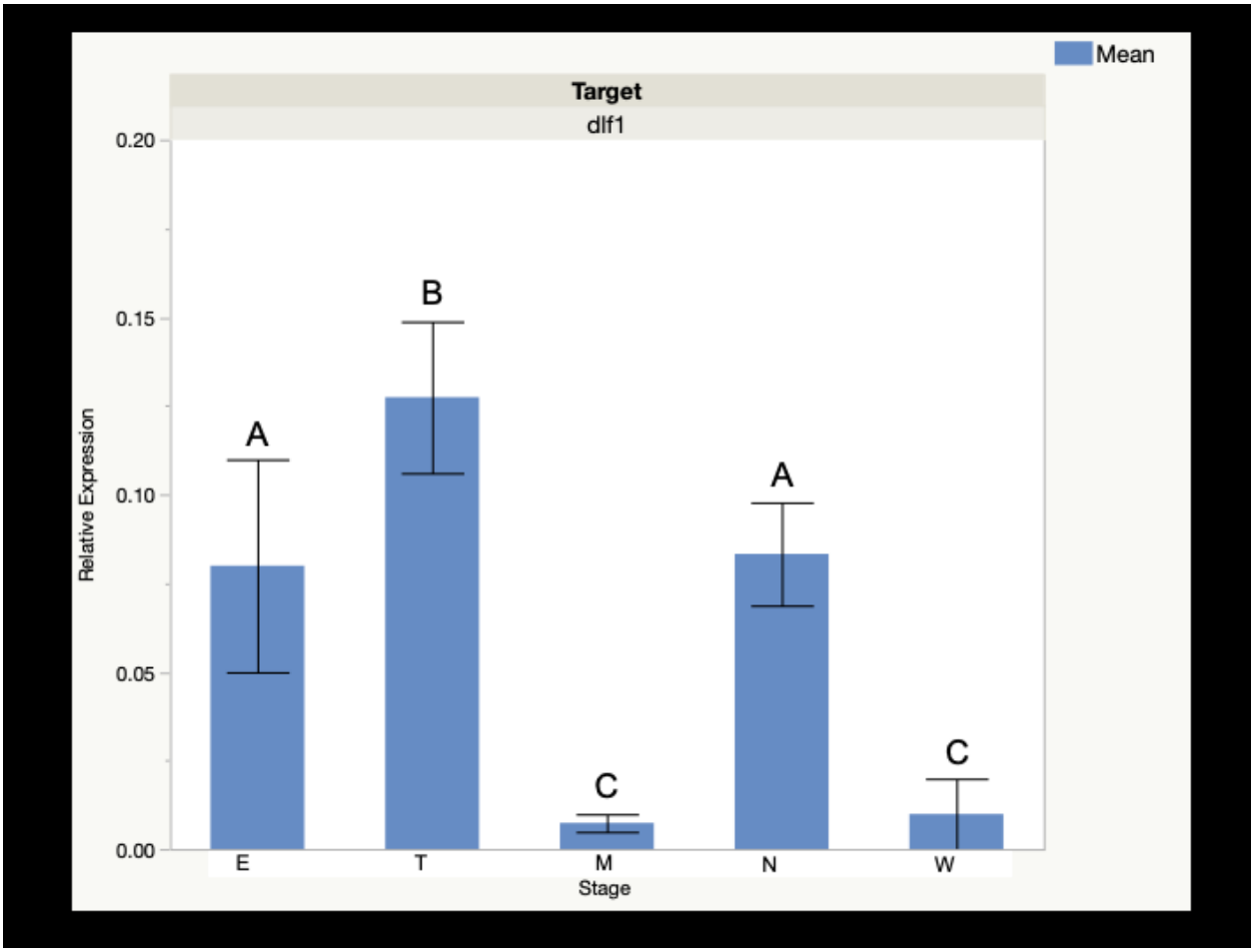

Figure 14. Relative expression data for *delayed flowering1* (*dlf1*) over developmental stages of the prong. Y-axis, relative expression; X-axis, developmental stages. E, emerging; T, transitioning; M, mature; N, no-prong; W, wild-type. Statistical significance was based on a multicomparison of the means, $P \leq 0.05$.

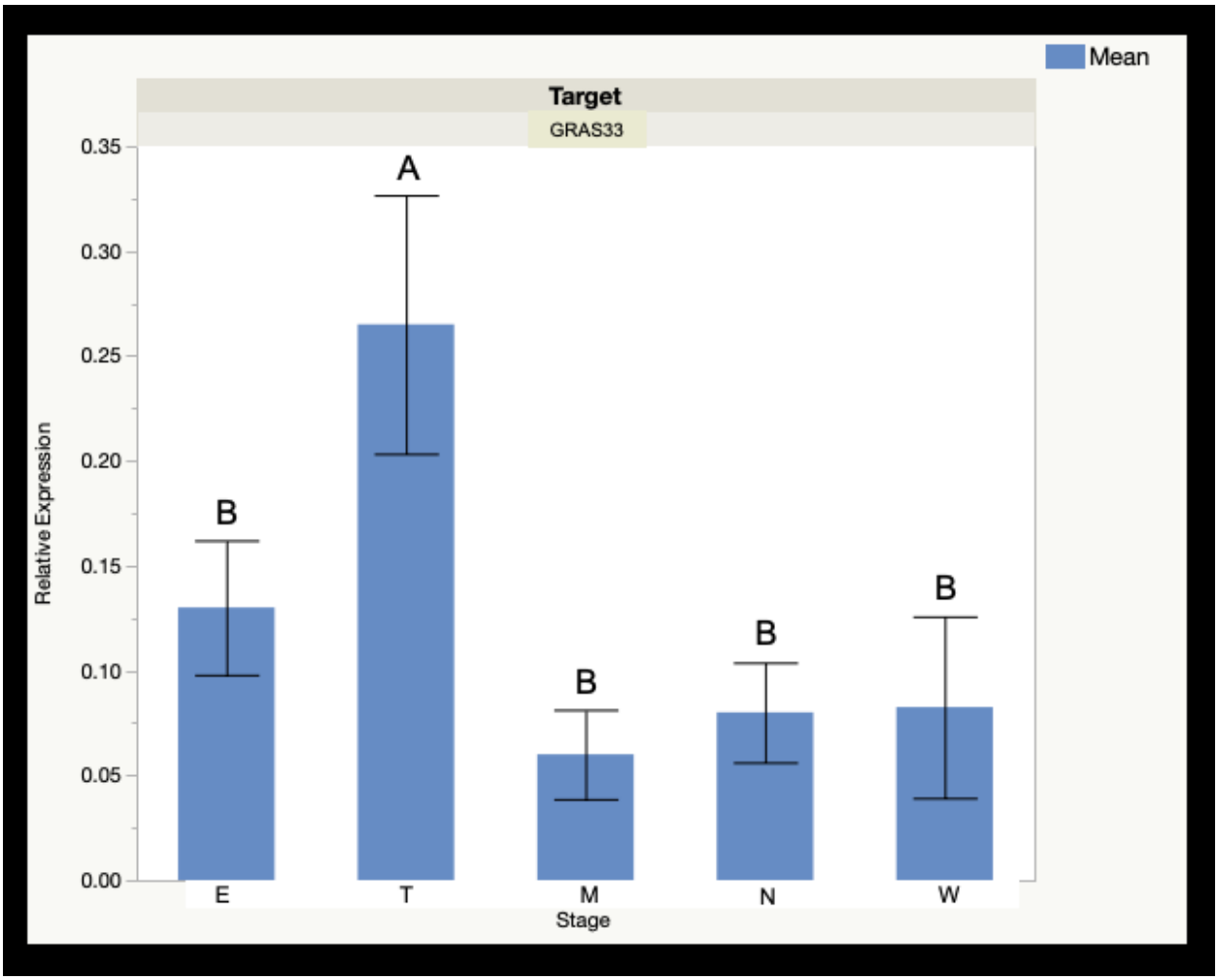

Figure 15. Relative expression data for *GRAS33* over developmental stages of the prong. Y-axis, relative expression; X-axis, developmental stages. E, emerging; T, transitioning; M, mature; N, no-prong; W, wild-type. Statistical significance was based on a multicomparison of the means, $P \leq 0.05$.

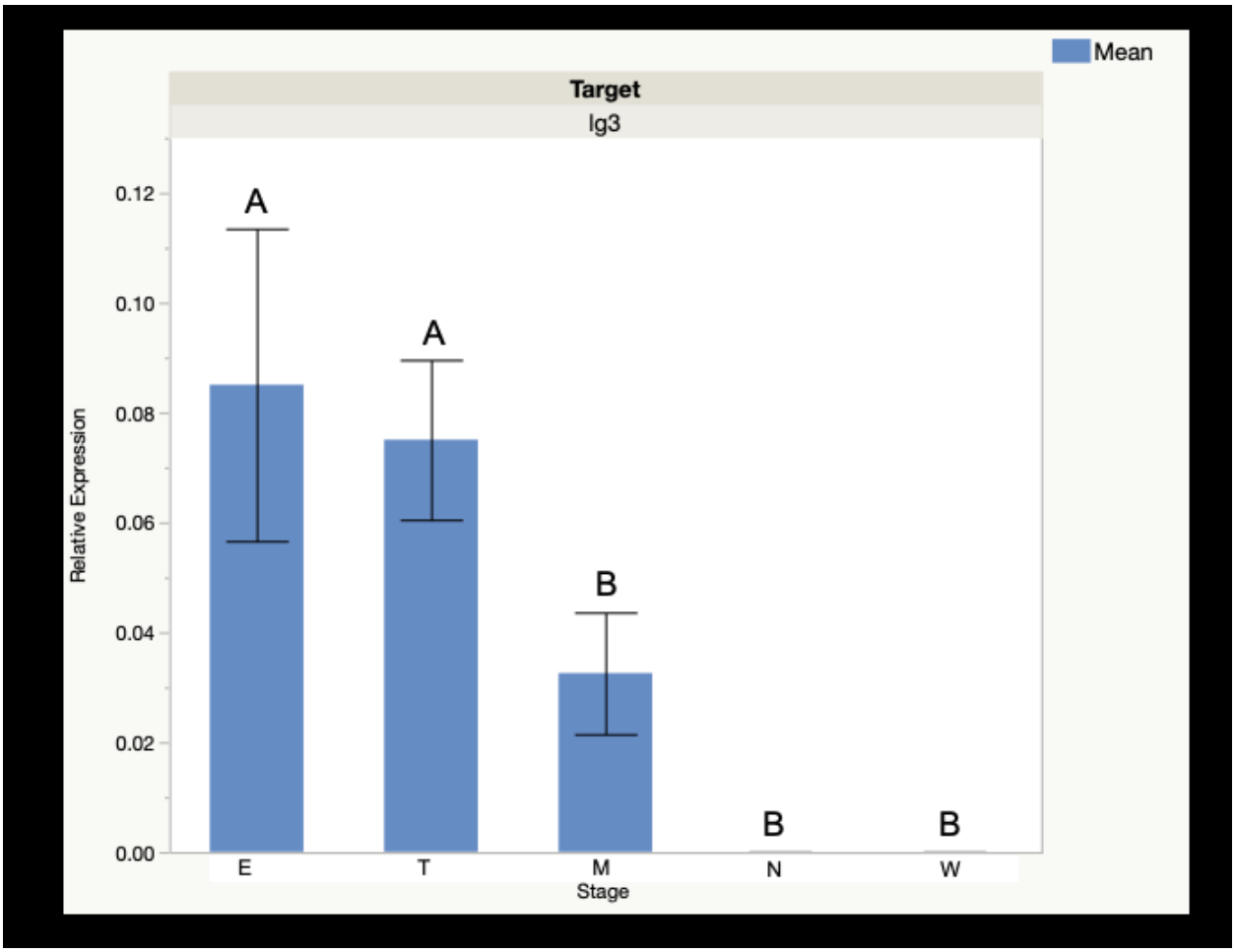

Figure 16. Relative expression data for *liguleless3* (*lg3*) over developmental stages of the prong. Y-axis, relative expression; X-axis, developmental stages. E, emerging; T, transitioning; M, mature; N, no-prong; W, wild-type. Statistical significance was based on a multicomparison of the means, $P \leq 0.05$.

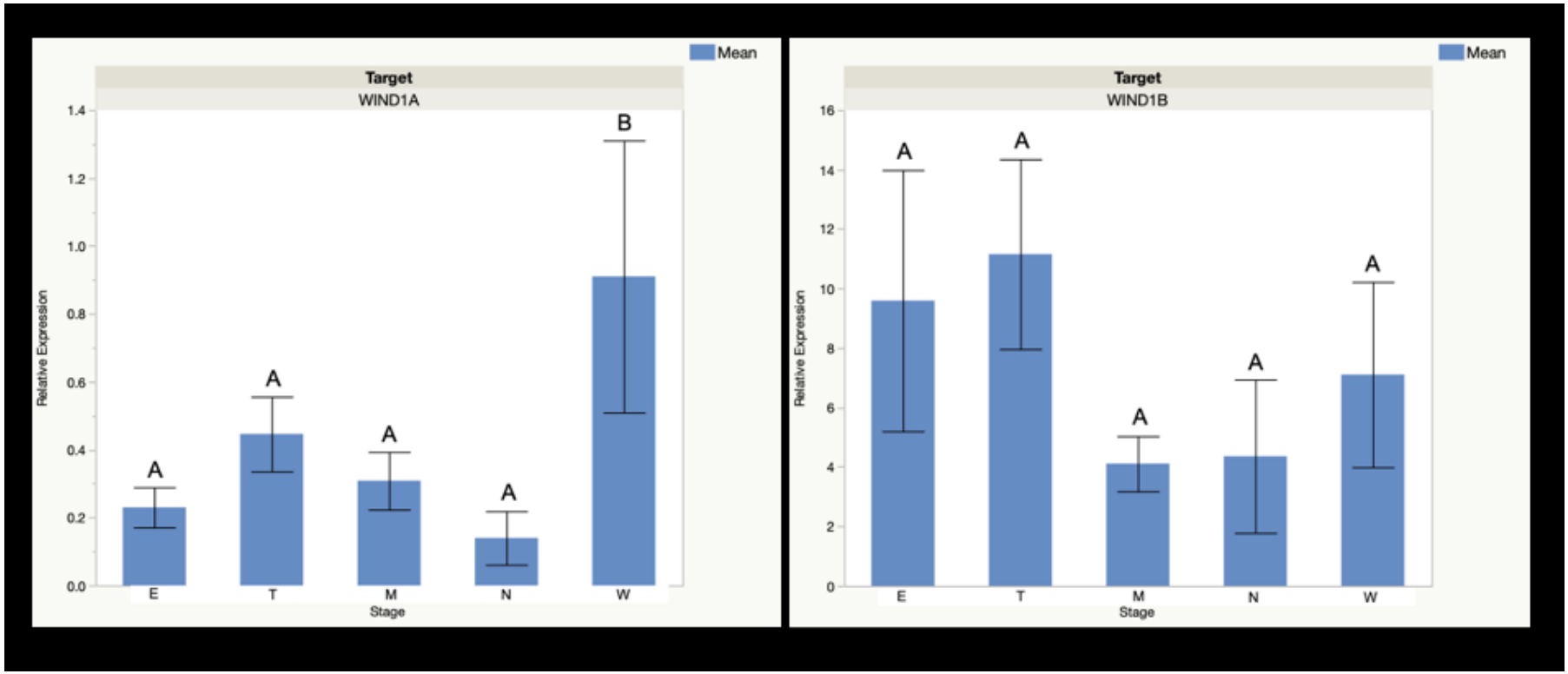

Figure 17. Relative expression data for the maize *WOUND INDUCED DEDIFFERENTIATION* (*WIND*) genes over developmental stages of the prong. (A) *ZmWIND1A* and (B) *ZmWIND1B*), Y-axis, relative expression; X-axis, developmental stages. E, emerging; T, transitioning; M, mature; N, no-prong; W, wild-type. Statistical significance was based on a multicomparison of the means, $P \leq 0.05$.

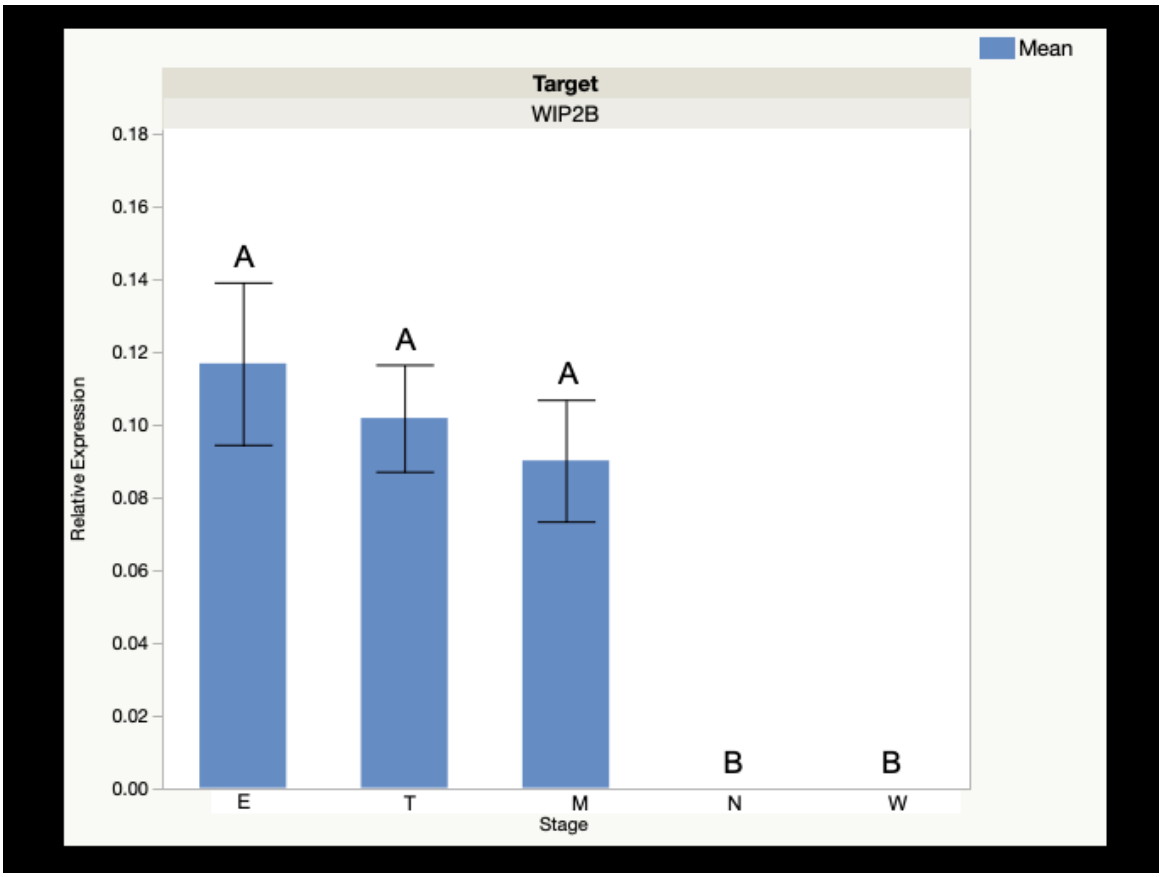

Figure 18. Relative expression data for maize *TRYPTOPHAN-ISOLEUCINE-PROLINE* (*WIP*) gene over developmental stages of the prong. (*ZmWIP2B*. Y-axis, relative expression; X-axis, developmental stages. E, emerging; T, transitioning; M, mature; N, no-prong; W, wild-type. Statistical significance was based on a multicomparison of the means, $P \leq 0.05$.

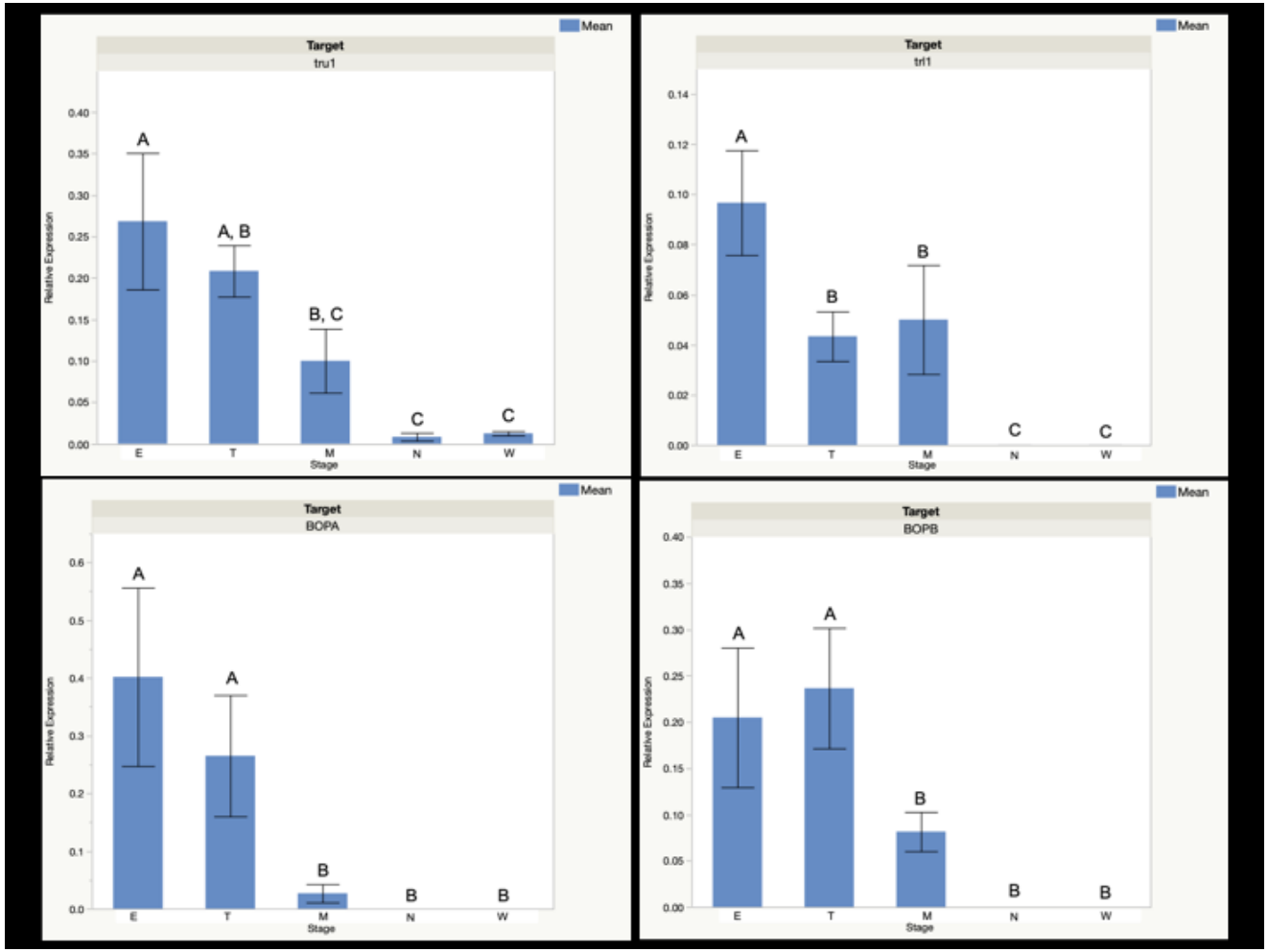

Figure 19. Relative expression data for the maize *BLADE-ON-PETIOLE (BOP*) genes over developmental stages of the prong. (Top-left) *tassel replaces upper ear1* (*tru1*), (Top-right) *tassel replaces upper ear- like1* (*trl1*), (Bottom-left) Zm*BOPA*, and (Bottom-right) *B* Zm*BOPB*. Y-axis, relative expression; X-axis, developmental stages. E, emerging; T, transitioning; M, mature; N, no-prong; W, wild-type. Statistical significance was based on a multicomparison of the means, $P \leq 0.05$.

Tables

Vial Name:	GRMZM2G######:	Sequence:	Tm (C):	Expected Size:
DCO0057	GRMZM2G029323	GTTGGCCCCAGATTCTTACA	60	105 bp
DCO0058		GACGAGTAGAGTGGCGGAAG	60	
DCO0059	GRMZM2G055204	AATACCAGCGCACACCAGAT	60	149 bp
DCO0060		GAATCTTGGGACATGGATGG	60	
DCO0065	GRMZM2G071101	GGCGGCGTCTCATCAGTA	60	214 bp
DCO0066		GCCCTCGCGTAGGAAGTC	60	
DCO0069	GRMZM2G445684	TCTGTTATTCGTGCCGATCC	60	98 bp
DCO0070		GCACCCAATAACGACAGCAT	60	
DCO0071	GRMZM2G067921	CTTCATCTCCACGCAGCTGAG	60	977 bp
DCO0072		CCCCAAAATGTCATTGTTCC	60	
DCO0073	GRMZM2G089619	CACAACCACAAGAACCAGCTC	60	216bp
DCO0074		CTAGACGCTGATGGGAGACG	60	
DCO0079	GRMZM2G328438	CGACGTACCACGAGTGTCTG	60	108bp
DCO0080		CTGCGCACTTGAGCCTGT	61	
DCO0081	GRMZM2G346920	GAGGAGATGACGCCGATG	60	106bp
DCO0082		CAGAATCCCCGTGCTTCG	62	
DCO0083	GRMZM2G414844	CTGACCTCTGGCTCGAACTC	60	325bp
DCO0084		GGCAGGAGCTTCATGTAGGA	60	
DCO0085	GRMZM5G821755	GTGTGGATGCACAACAACAAG	60	171bp
DCO0086		GTCGGTCACTCCAAGTCCAG	60	
DCO0087	GRMZM2G039867	ATGATGGTGAGATAATCCGTTTG	60	204bp
DCO0088		CTCTTAAAATGTCCCAGACAACG	60	
DCO0089	GRMZM2G022606	CTCCAAAACCCGCCTTCT	60	209bp
DCO0090		CCAGCGAGAGGGACTTGA	60	
DCO0091	GRMZM2G060723	GCCGGCTGCTGCTCTACT	61	120bp
DCO0092		TCGTCTCGCCATCTTTCC	59	
DCO0093	GRMZM2G026556	ATACATACACAGTTGCGTTGTCG	60	210bp
DCO0094		TGCCTTCCCTTTATATTTTCTGG	60	
ARV0167	GRMZM2G079470	ACAACAGCCAAGCGCTATCT	60	230 bp
ARV0168		GAGTCGTATCCGCTCTGGAC	60	

Table 2. Primer information for genes of interest. Primer pairs were designed based on the respective cDNA sequence from MaizeGDB version 4. First column represents the primer ID for the primer, second is target allele. Following those columns are the primer sequence, optimal annealing temperature (C), and finally the expected fragment size (bp).

	# of prongs	A	B	C	D
Emerging	36	76%	21%	3%	0%
Transitioning	28	92%	8%	0%	0%
Mature	25	57%	43%	0%	0%

Table 3. Prong distribution by each developmental stage. The first and second column list each prong stage and the number of prongs found at that stage. A-D correspond to Figure 13 and the quadrants. The percentages are calculated from the total number of prongs of each stage found within each quadrant divided by the total number of prongs X 100.

Objective 2 - EPISTATIC ANALYSIS of *Hsf1*

Introduction

This project prioritized a number of DE genes that had a significant fold-change increase in initiating prongs and known or presumed role in organogenesis. I hypothesized that these DE genes have a function in prong formation and also can influence leaf patterning. Expression analysis of these DE genes throughout prong development either supported the presumed role for a gene in prong formation or not. To further clarify the function of a few of these DE genes, I performed double mutant analysis with a DE gene and *Hsf1*/+. The idea is that if the expression of the DE gene contributes to prong formation, loss of that function due to a recessive mutation for the DE gene, when combined with *Hsf1*/+ will affect the prong phenotype. If the DE gene promotes prong formation, loss of that activity will lead to smaller or fewer prongs in the double mutant with *Hsf1*/+. This technique will allow me to quantify the epistatic interaction of the targeted DE gene with *Hsf1* by measuring the degree of phenotypic variation between the *Hsf1*/+ single and double mutants.

An example of this was shown using the*lg3* gain-of-function mutant, *Lg3-O.* Since *lg3* was highly expressed in initiating *Hsf1*/+ prong tissue, it is expected that if there more *lg3* was added to the system, a change in prong phenotype would occur. To quantify the change in prong formation, a measurement of how much margin consists of prong tissue was developed wherein the length (P-D) of each prong was measured, summed for all prongs on a leaf, and divided by the approximate length of the leaf margin. This measurement of percent prong margin (PPM) allowed for precise

quantification of any changes in prong development, [Figure 22]. When the *Hsf1*/+ mutation was combined with the *Lg3-O/+* mutation, the size of the prongs and PPM increased dramatically (Muszynski et al., unpublished). This suggested that *lg3* is not only a meristem maintenance gene but also is needed for the formation of prongs.

The dlf1 gene encodes a bZIP TF that promotes the floral transition by interacting with the mobile floral signal ZCN in the shoot apex (Muszynski et al., 2006). The loss-of-function *dlf1* mutant, shows a prolonged vegetative state of approximately one to two weeks, resulting in taller plants with more leaves.

The *tassel replaces upper ear1* (*tru1*) gene is a homolog of *BLADE-ON-PETIOLE1* (*BOP1*) in *Arabidopsis,* and other BOP-family genes have been identified in the prong RNA-seq dataset to be DE. *BOP1* encodes a BTB/POZ protein that is known to repress class I *KNOX* genes during leaf initiation (Dong et al., 2017). More importantly, *BOP1* and related genes influence leaf patterning by regulating cellular identities in the developing leaf.

Materials and Methods

Plant Material

Hsf1-1603 is the allele used in this research and is referred to as *Hsf1* throughout this thesis. *Hsf1-1603* was produced by EMS mutagenesis treatment of the inbred line Mo17. *Hsf1-1603* was backcrossed to B73 more than ten generations and this is the material used in my thesis research unless otherwise noted. Because homozygotes of *Hsf1* are lethal, all the analyses were performed using the heterozygote class. The *delayed flowering1 (dlf1)* mutant used in this study was also introgressed into B73. The *tassel replaces upper1* (*tru1*) mutant was obtained from Dr. George Chuck (University of California, Berkley) and was introgressed into the inbred line A619. Double mutants were produced by crossing homozygous recessive mutants (*dlf1* or *tru1*) to *Hsf1*/+, then selecting progeny *Hsf1*/+ plants which were heterozygous for the recessive mutation, and backcrossing those by their respective recessive mutant lines. The resulting double mutant families segregated: 25% +/+, +/-, 25% *Hsf1*/+, +/-, 25% +/+, -/-, and 25% *Hsf1*/+, -/- (where the "-" represents the recessive mutant allele of interest) [Figure 20]. For the *tru1* study, the *Hsf1*/+ mutants, originally from the B73 background, were introgressed into the A619 inbred background more than 10 doses before crossing with *tru1* [Figure 21].

Growth Conditions

Seeds were treated with Baytan® T to prevent mold and fungal growth. Plants were started in 32-well growing flats in the William T. Pope Greenhouse at the University of Hawai'i- Mānoa (Honolulu, HI). Seedlings were transplanted into 3-gallon

pots once fifth leaf emerged and leaf four was fully collared. The fifth leaf was marked to track leaf number as the plant matured.

Leaf Measurements

Leaves were removed when the plant began to tassel and then measurements were taken for leaf length, leaf width, and percent prong margin (PPM) [Figure 22]. Leaf length is defined as the distance between the most proximal point of the blade, the blade-sheath boundary, and the distal tip of the leaf. Leaf width is the distance between margins at half of the leaf blade length. PPM, which is the percentage of the blade margin that consists of prong tissue, is a two-part measurement. First, each individual prong is measured along the margin of each leaf. All those length values are added together to equal total prong length for each leaf. Second, leaf length is multiplied by two, because both sides of the blade is comprised of margin tissue. Finally, the PPM is the proportion of total prong length coverage divided by the total margin length multiplied by 100 [Figure 22].

Statistical Analyses

The experimental design was a completely random design with three replicates. Statistical analyses were done using JMP Pro (v.13) software developed by the SAS Institute. An analysis of variance (ANOVA) was conducted followed by a Tukey's HSD multiple comparison for the means. Tukey's HSD was used to analyze the leaf length, leaf width, height, and sheath length among all genotypes of the same population.

Genotyping Assays

Gene specific primer pairs were designed using Primer3 (Untergasser et al., 2012) for each target gene using the publicly available maize genome (Version 3,

Portwood et al., 2018) through MiazeGDB (Portwood et al., 2018). Gene structure was analyzed through Gramene (B73_RefGen_v4) to identify translated and untranslated regions of the transcript.

All plants from populations that segregate *Hsf1/+* were genotyped for *Hsf1* with oligos ARV0123 and ARV0124 [Table 4]. Expected band size are1010 bp for wild-type B73, and 1345 bp for *Hsf1*.

All plants from populations that segregated *dlf1* mutants were genotyped for *dlf1* using a Cleaved Amplified Polymorphic Sequences (CAPs) assay using oligos DCO0045 and DCO0046 [Table 4] followed by $B_5sS^{\alpha}I$ digestion. PCR amplification products were incubated at 37ºC for 1 hour before running on a 1% agarose gel. The PCR product from the *dlf1* allele has the $B_5sS^{\alpha}I$ site and so the mutant allele resolves itself into bands of 328 and 649 bp, while the wild type allele produces a single band of 977 bp. A result of all three bands would indicate the plant was heterozygous for the *dlf1* mutant allele.

All plants from populations that segregate *tru1* mutants were genotyped for *tru1* using oligos ARV0229 and ARV0230 [Table 4].

PCR reactions were set up using EconoTaq® PLUS GREEN 2X Master Mix (Lucigen) following manufacturers recommendations and annealing temperatures are designated in Table 1. Each reaction was run on a S1000 Thermocycler and then PCR amplification products were run on a 1% agarose gels.

Results

Hsf1/+, *dlf1/dlf1* double mutants produce fewer prongs than *Hsf1*/+ single mutants

The *dlf1* gene has not been associated with a role in leaf patterning or organ formation although it is expressed in immature leaves surrounding the shoot apex. However, RNA-sequencing showed that *dlf1* had a six-fold change in expression in the prong tissue compared to the wild-type and no-prong [Figure 23A], suggesting a possible mechanistic role in prong formation.

Crossing the *Hsf1* mutation with *dlf1* mutants provided the expected segregations [Table 5]. The *dlf1* single mutant does not produce any prongs [Figure 23B]. As expected for a late flowering mutant, the *Hsf1/+, dlf1* double mutant plants produced twenty-two to twenty-eight leaves, while the *Hsf1/+* single mutant plants produced a maximum of nineteen leaves. This did not allow for a leaf by leaf analyses as was possible in the *lg3* epistasis study. For consistency, percent prong margin (PPM) and other leaf measurements were taken from the leaf subtending the top ear and the remaining leaves up to the tassel. The *Hsf1/+* single mutant had a higher PPM on average in comparison to the *Hsf1/+, dlf1* double mutant [Figure 23C]. The PPM gradually increased as leaf number increased in the *Hsf1/+* single mutant, as was seen before. However, this trend was not seen in the double mutant, where there was a significant overall reduction in PPM for all leaves, staying in the range of 4-10%.

Making crosses for *tru1* was difficult as homozygous *tru1* female plants could not be used as pollen recipients due to the tassel replacing the upper ear phenotype. The introgression of *Hsf1/+* into *tru1* in the A619 background produced the expected 1:2:1 segregation [Table 6]. Since the purpose of these crosses were to produce double

mutants, the presence of an enhanced *Hsf1*/+ phenotype reduced by 50% the number of Hsf1 plants that could be grown to maturity. In the end, I did not recover any double *Hsf1*/+, *tru1/tru1* mutants, even though the expected segregation ratio was seen for *Hsf1*/+, +/+ and *Hsf1*/+, *tru1*/+ genotypes.

Discussion

The semi-dominant *Hairy sheath frayed1* (*Hsf1*) is due to gain-of-function missense mutations in the *Zea mays Histidine Kinase* (*ZmHK1*) cytokinin receptor. The *Hsf1* mutation causes the receptor to be hyperactive or hypersignaling. The *Hsf1* mutant produces ectopic tissue in the leaf margin that are called prongs and RNA-seq studies in prongs have determined that key transcription factors are upregulated during prong initiation.

A few of these DE genes are that are TFs also have mutants available. These were obtained and were crossed to *Hsf1* to measure their loss-of-function effects on prong formation. Double mutant analysis with *dlf1* and *Hsf1* indicated that *dlf1* contributes to the development of prongs. In the *Hsf1/+, dlf1* double mutants, the PPM is significantly decreased compared to the single mutant, *Hsf1/+, dlf1/+*. Similarly, to *dlf1* single mutant, the *Hsf1/+, dlf1* double mutants had a prolonged vegetative state, resulting in the production of more leaves than the *Hsf1/+* single mutant. Since the *Hsf1*/+, *dlf1*/*dlf1* plants produced more leaves, similar to the +/+, *dlf1*/*dlf1* plants, I was not able to make a leaf by leaf comparison of PPM. But graphing the PPM for all the leaves about the top ear for each genotype revealed a trend in the *Hsf1* single mutants. As leaf number increased, PPM increased too. Loss of *dlf1* function removed this trend. This result suggests that *dlf1* does promote prong formation, potentially by increasing PPM in the uppermost leaves of the shoot. How this positional information in perceived and signaled is an area for future studies.

Using similar methods, it would be expected that *Hsf1/+, tru1* double mutants might reveal similar trends as seen with the *dlf1* mutation. Due to the presence of a genetic

Hsf1 enhancer fixed in the A619 inbred line and background for tru1, analysis of *Hsf1/+, tru1/tru1* double mutants will require a much larger population to be grown in order to obtain enough double mutant plants for phenotypic analysis.

Future Directions

Double mutant analyses have shown to be a useful strategy in determining the role of the of identified DE genes in prong development and leaf patterning. Further studies will need to be conducted with the other DE genes, where crossing of *Hsf1* into the mutant line may require the creation of mutants by means of new mutagenesis, or gene-editing using CRISPR-Cas9 transgenics. Currently, *tassel replaces upper ear1 (tru1)* has been crossed with *Hsf1/*+ plants, resulting in a *Hsf1/*+*, tru1* double mutants [Figure 21]. For further analysis, *tru1* double mutants will require leaf analyses, including percent prong margin, for comparison with *Hsf1/*+ plants.

Figure Legends

Figure 20. Crossing of *Hsf1/+* with the recessive loss-of-function *delayed flowering1* (*dlf1*) mutant. Crosses took place in the B73 inbred background to produce double mutants. Progeny resulted in four segregating genotypes with a 1:1:1:1 ratio. Double mutants, *Hsf1/+, dlf1/dlf1*.

Figure 21. Crossing of *Hsf1/+* with the recessive loss-of-function *tassel replaces upper-ear1* (*tru1*) mutant. Crosses took place in the A619 inbred background to produce double mutants. First cross resulted in four segregating genotypes with a 1:1:1:1 ratio. Second sib cross resulted in six segregating genotypes with a 1:2:1 ratio. Double mutants, *Hsf1/+, tru1/tru1*.

Figure 22. Method of measuring percent prong margin (PPM) per leaf. Prong length are marked by the red brackets. Twice the leaf length is shown by the yellow dotted arrow. Equation used to calculate PPM is shown at the bottom of the figure.

Figure 23. The *delayed flowering1* (*dlf1*) gene is upregulated in prongs and influences prong size. (A) *dlf1* is upregulated in initiating prongs. (B) Loss of *dlf1* function in the recessive mutant leads to late flowering but does not affect leaf morphology. Combined with *Hsf1/+*, double mutants have smaller and fewer prongs (red circles). (C) Average percent prong margin is lower in *Hsf1/+, dlf1/dlf1* plants with standard error bars.

Figure 24. The *dlf1* mutant inhibits the increase in PPM in the upper leaves of *Hsf1*. (A) Percent prong margin (PPM) is correlated to leaf number in the *Hsf1/+* single mutant. PPM increases as leaf number increases. (B) PPM does not seem to be correlated with leaf number in the *Hsf1/+* double mutant. Red line denotes top ear position in each genotype.

Figures

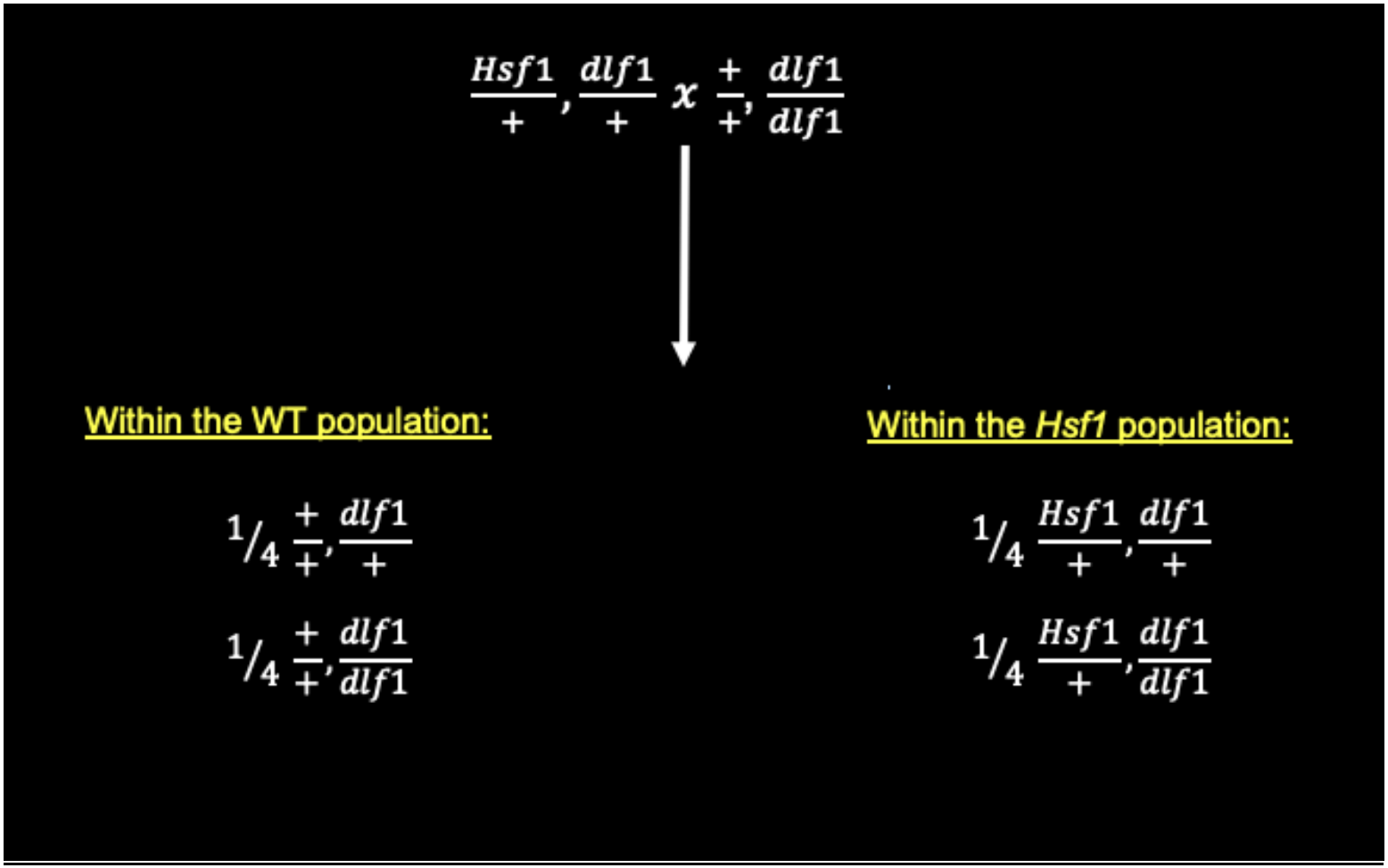

Figure 20. Crossing of *Hsf1*/+ with the recessive loss-of-function *delayed flowering1* (*dlf1*) mutant. Crosses took place in the B73 inbred background to produce double mutants. Progeny resulted in four segregating genotypes with a 1:1:1:1 ratio. Double mutants, *Hsf1*/+, *dlf1/dlf1.*

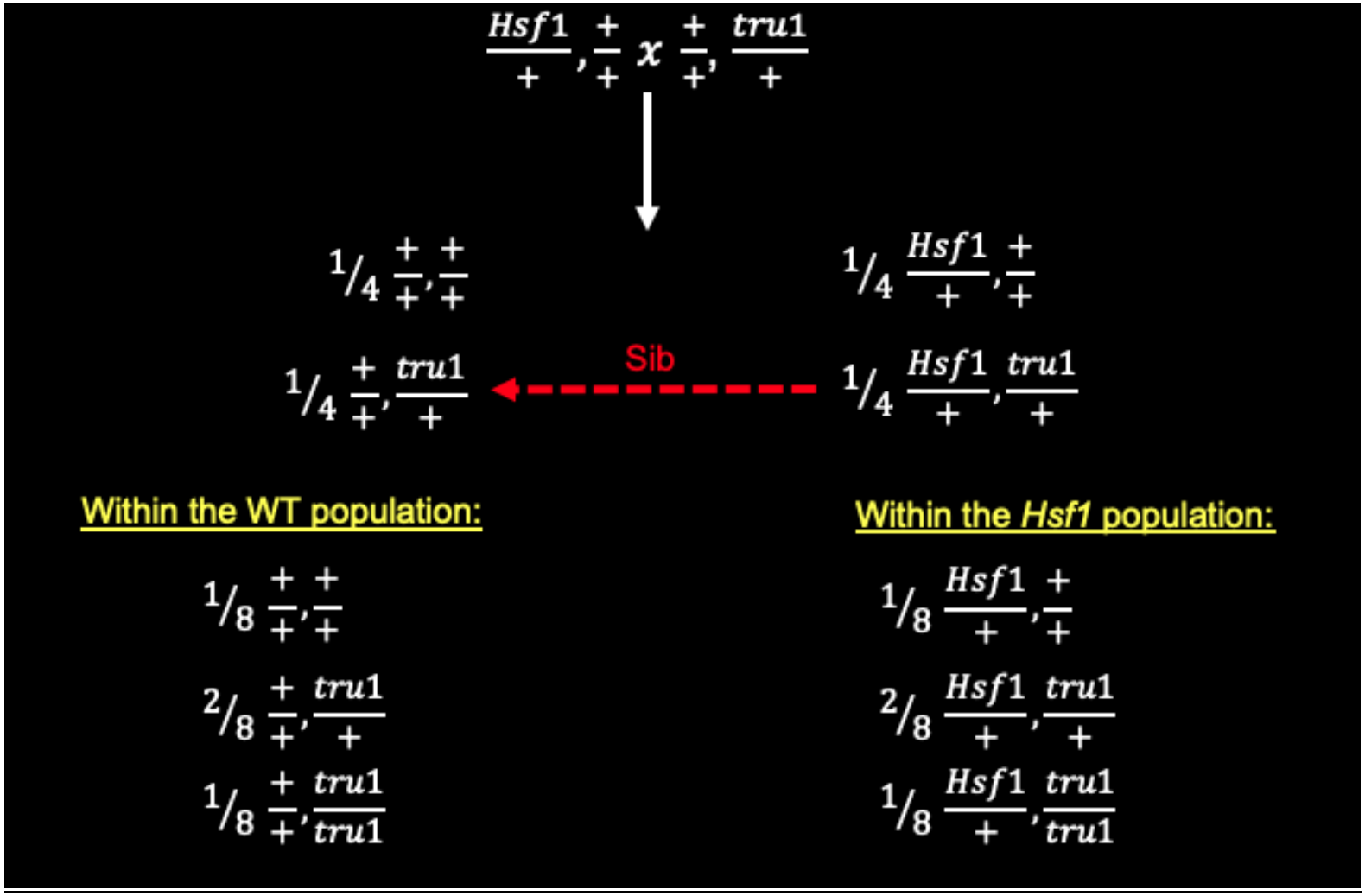

Figure 21. Crossing of *Hsf1*/+ with the recessive loss-of-function *tassel replaces upper-ear1* (*tru1*) mutant. Crosses took place in the A619 inbred background to produce double mutants. First cross resulted in four segregating genotypes with a 1:1:1:1 ratio. Second sib cross resulted in six segregating genotypes with a 1:2:1 ratio. Double mutants, *Hsf1/+, tru1/tru1.*

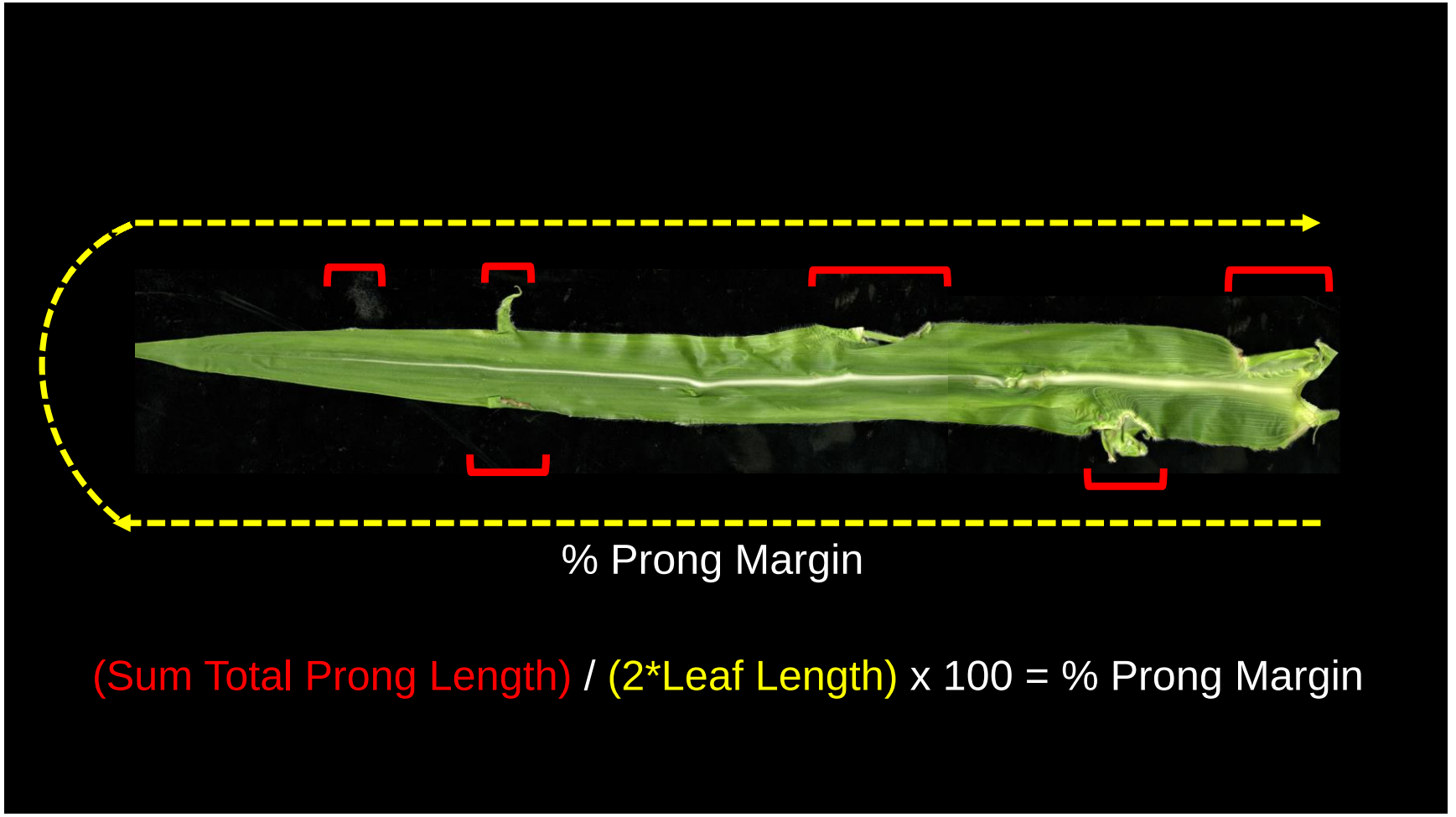

Figure 22. Method of measuring percent prong margin (PPM) per leaf. Prong length are marked by the red brackets. Twice the leaf length is shown by the yellow dotted arrow. Equation used to calculate PPM is shown at the bottom of the figure.

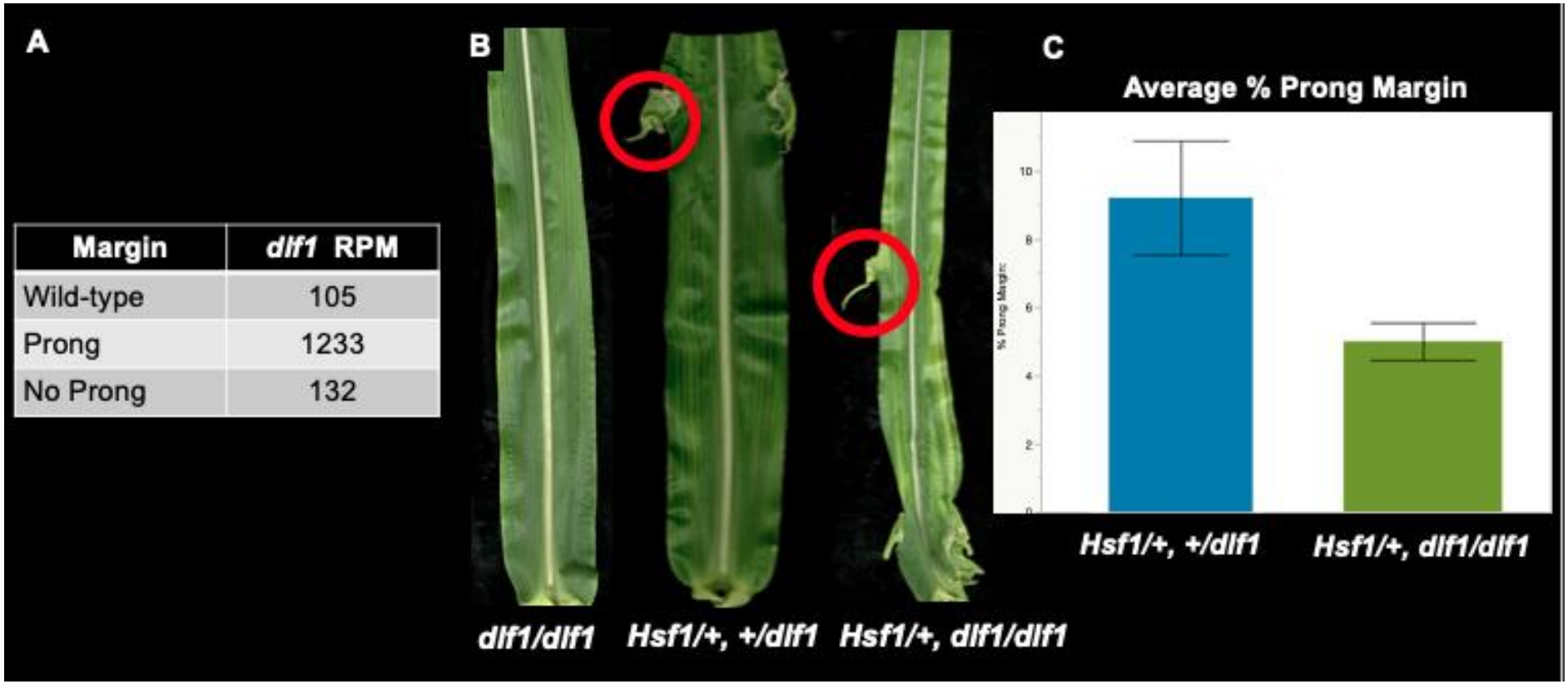

Figure 23. The *delayed flowering1* (*dlf1*) gene is upregulated in prongs and influences prong size. (A) *dlf1* is upregulated in initiating prongs. (B) Loss of *dlf1* function in the recessive mutant leads to late flowering but does not affect leaf morphology. Combined with *Hsf1/+*, double mutants have smaller and fewer prongs (red circles). (C) Average percent prong margin is lower in *Hsf1/+, dlf1/dlf1* plants with standard error bars.

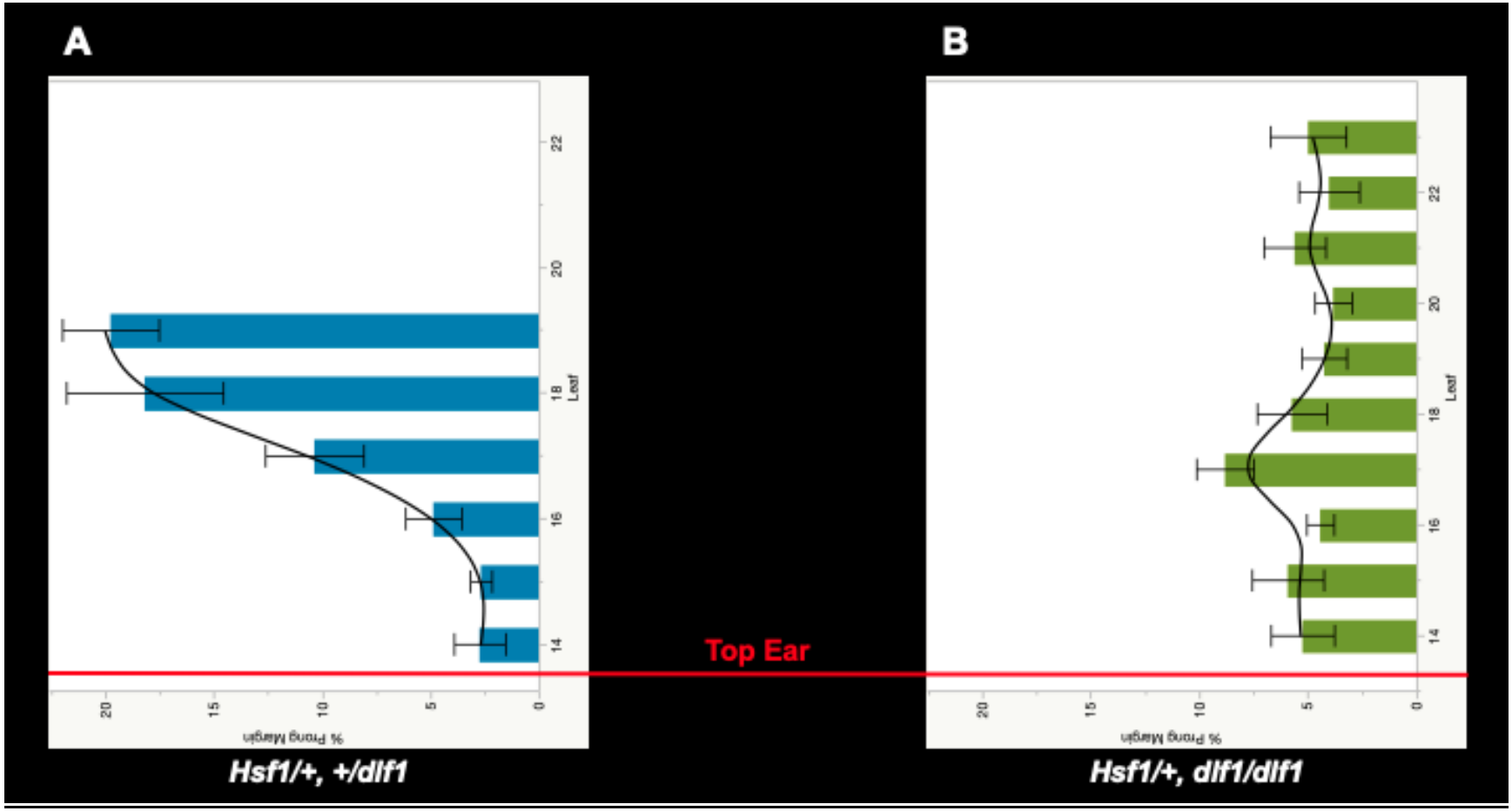

Figure 24. The *dlf1* mutant inhibits the increase in PPM in the upper leaves of *Hsf1*. (A) Percent prong margin (PPM) is correlated to leaf number in the *Hsf1*/+ single mutant. PPM increases as leaf number increases. (B) PPM does not seem to be correlated with leaf number in the *Hsf1*/+ double mutant. Red line denotes top ear position in each genotype.

Tables

Primer Name	Target	Primer Sequence	Expected Size	Tm (C)
ARV0123F	*Hsf1*	GCCACACTGAAGCACTCATA	B73=1010 bp	58
ARV0124R	*Hsf1*	CAGCCGCAGCAACTCTGAGG	Mo17=1345 bp (Hsf1)	58
DCO0045F	*dlf1*	CTTCATCTCCACGCAGCTGAG	977 bp	60
DCO0048R	*dlf1*	CCCCAAAATGTCATTGTTCC		60
ARV0229F	*tru1*	AAGAGAGGGGCCTGACGTTC	306 bp = WT	60
ARV0230R	*tru1*	CCTGCTCGGTTTCTTTGCTAGTG	>300 bp = MU	60

Table 4. Genotyping primers. Table includes the primer direction (F, forward; R, reverse), target gene, primer sequence, expected fragment size if ran on a gel, and optimal annealing temperature.

Genotype	Expected	Observed	Total	P-value
[+/+, *dlf1*/+]	11	7	**43**	**0.50855**
[+/+, *dlf1/dlf1*]	11	8		
[*Hsf1*/+, *dlf1*/+]	11	16		
[*Hsf1*/+, *dlf1/dlf1*]	11	12		

Table 5. Segregation results of crossing *Hsf1*/+ into *delayed flowering* (*dlf1*). First column shows the four expected segregating genotypes. Second and third columns provide the expected number of plants and the observed number plants for each genotype. Fourth column provides the total number of plants produced during the study. Chi-square with a confidence interval of 95% was used to determine if the observed segregation fit the expected segregation with a p-value. $P \geq 0.05$.

Wild-type				
Genotype	Observed	Expected	P-Value	Segregation
[+/+, +/+]	7	7	0.677172	1:2:1
[+/+, tru1/+]	15	14		
[+/+, tru1/tru1]	4	7		
Mutant				
Genotype	Observed	Expected	P-Value	Segregation
[Hsf1/+, +/+]	5	3	0.460621	1:2:1
[Hsf1/+, tru1/+]	5	6		
[Hsf1/+, tru1/tru1]	1	3		

Table 6. Segregation results of crossing *Hsf1/+* into *tassel replaces upper-ear1* (*tru1*). Top half, wild-type population, bottom half, *Hsf1/+* population. First column shows the three expected segregating genotypes. Second and third columns provide the expected number of plants and the observed number plants for each genotype. Fourth column is the calculated chi-square p-value with a confidence interval of 95% used to determine if the observed fits the expected segregation ratio at a p-value. $P \geq 0.05$. Last column is the expected segregation ratio.

OBJECTIVE 3 - NOVEL PHENOTYPE: ENHANCER LOCUS CHARACTERIZATION

Introduction

Hsf1/+ is a semi-dominant mutant, therefore when *Hsf1*/+ is crossed to an inbred line we expect a 1:1 segregation ratio between the wild-type (+/+) and mutant (*Hsf1*/+) phenotypes. *Hsf1*/+ was introgressed for more than 8 generations in to several standard inbreds, including the inbred A619. This was to facilitate phenotypic analysis of *Hsf1* and crossing the mutant to other mutants that exist in different inbred backgrounds. Observation of the *Hsf1* phenotype in the inbred line A619 showed the expected 1:1 segregation between wild-type and *Hsf1*/+ mutants. However, in the *Hsf1*/+ class I observed that 50% had the standard *Hsf1*/+ phenotype, while the other 50% produced an enhanced *Hsf1*/+ phenotype [Figure 24]. The enhanced *Hsf1* phenotype resembled to a large extent when *Hsf1*/+ was combined with the *aberrant phyllotaxy1 (abph1)* double mutants, which produced multiple shoots [Figure 25]. The enhanced phenotype was only seen within the *Hsf1*/+ population and did not show any phenotypes in the WT plants. I observed this same segregation in growing out samples from multiple A619 backcross sources from different years. I hypothesize that a genetic enhancer is segregating in these families that behaves as a single recessive modifier, because I only see the enhanced phenotype in half of the *Hsf1*/+ population. To test my hypothesis, I conducted a series of crosses to determine if the genetic enhancer behaves in a recessive fashion. Since the underlying gene is unknown, I was not able to generate a genotyping assay to distinguish the WT plant containing the enhancer allele. For the purpose of the progeny tests, I sib crossed many standard *Hsf1*/+ plants to many viable WT sib plants this is because the enhanced *Hsf1* plants were sterile in the

greenhouse and have a 100% mortality in the field. Due to this factor, the enhancer locus was maintained by unknowingly crossing *Hsf1*/+ plants heterozygous for the enhancer locus.

Materials and Methods

Genetic Stock

Hsf1-1603 was backcrossed for 10 or more generations into the A619 inbred in the field using *Hsf1/+* plants that were fertile and this had the standard *Hsf1* phenotype.

Growth Conditions

Seeds were treated a 24-hour treatment of Baytan® T (Bayer) to prevent mold and fungal growth. Plants were started in 32-well growing flats in the William T. Pope greenhouse (University of Hawai'i at Mānoa). Seedlings were then transplanted into 3-gallon pots until five leaves were visible. The fifth leaf was marked for record keeping, as the first four leaves senesce completely before the plant reaches maturity.

Enhancer Determination Strategy

A 1:1 segregating population of *Hsf1/+* in the A619 background was planted and the phenotypes recorded. Standard *Hsf1/+* and wild type sibs were grown to maturity and were intercrossed to maximize crossing between different individual plants. This developed the segregating populations to test the segregation of the enhancer locus [Figure 26]. If the enhancer locus segregates as a single recessive locus, and the A619 inbred is fixed for the enhancer allele while the standard *Hsf1* plants are heterozygous for the enhancer allele, then two outcomes are expected in the progeny of sib crossing. The progeny of sib crosses is expected to segregate 3:1, if the WT sib was heterozygous for the enhancer allele, and 1:1 if the WT sib was homozygous for the enhancer allele. The progeny segregating 3:1 has three genotypes for the *Hsf1* class: [*Hsf1*/+, +/+], [*Hsf1/+, enh/*+], and [*Hsf1/+, enh/enh*], while the progeny segregating 1:1 has two genotypes for the *Hsf1* class: [*Hsf1/+, enh/*+] and [*Hsf1/+, enh/enh*].

Statistical Methods

Deviation from the expected segregation was determined via the chi-square method. Expected segregation ratios and construction of the two models were determined using Mendelian segregation method for diploid species.

Results

Discovery of a genetic enhancer of *Hsf1* in the A619 inbred background

The A619 inbred background produced a unique phenotype among the *Hairy sheath frayed1* (*Hsf1*) population. It was observed that the segregation between *Hsf1*/+ to wild-type sibs still followed the expected 1:1 segregation, however within the mutant population, there was a 1:1 segregation ratio between a ‘standard’ and ‘enhanced’ *Hsf1.* Enhanced *Hsf1* plants showed multiple shoots, twin embryos, decreased internode length, and most of the time did not reach a reproductive state.

Enhanced plants were not observed in the field and led us to hypothesize that it may be lethal; either due to their slower growth rate or abnormal vegetative growth. As a result, the heterozygote state for the enhancer allele was selected unintentionally, since backcrossing in the field could only be done with viable, fertile *Hsf1* plants..

Close inspection of the plants that produced multiple shoots determined that the extra shoots had modified leaves and tubular organs. The cells that make up the sheath failed to differentiate into two margins and stayed fused [Figure 27A&B]. Twin embryos refers to the planting of one seed and having two plants germinate. Dissection of the twin plants showed that these arose from a single root system and were not due to two embryos in 1 seed [Figure 27C].

Crossing Schemes for Enhancer Locus Validation

To determine if the genetic action of the enhancer was due to a single recessive locus, as was suggested by the 1:1 segregation of standard *Hsf1* to enhanced *Hsf1*, I chose to do two different progeny tests. The first progeny test was to identify whether the enhancer segregated as a single recessive locus. This was tested by crossing

Hsf1/+ heterozygous for the enhancer allele to WT plants in the A619 background. By doing so, I crossed all the standard *Hsf1*/+ plants to the WT population, because I did not have a genotyping assay for the enhancer gene. I hypothesized that by doing this I would be crossing WT plants that were either heterozygous or homozygous for the enhancer allele, which would result in two different segregation genotypes. I expected that if the standard *Hsf1*/+ plants were sib crossed to the WT plants heterozygous for the enhancer, the progeny would segregate 3:1 (standard: enhanced). However, if I were to sib cross to the WT plants homozygous for the enhancer, I would expect the progeny to segregate 1:1 (standard: enhanced). My results for eight sib crosses produced either a 1:1 or a 3:1 segregation [Table 7].

To validate this result, I conducted a second progeny test only using the progeny that segregated 3:1. My hypothesis was, if the genetic enhancer is due to a single recessive locus, then some of the plants in the 3:1 segregating family would not have the enhancer allele, and sib crossing would uncover this. Using the standard *Hsf1*/+ plants, either *Hsf1*/+ without or heterozygous for the enhancer allele, I crossed to all possible WT sibs. Again, since I did not have a genotyping assay for the enhancer gene, I proposed that among the WT population there should be three genotypes, (1) without the enhancer, (2) heterozygous for the enhancer, or (3) homozygous for the enhancer allele. I would expect that crossing the two genotypes of standard *Hsf1*/+ with the three genotypes in the WT population would result in six segregating genotypes. However, overall there will be three distinct segregation classes. The first class would come from sib crossing the *Hsf1*/+ plants that did not contain the enhancer allele to all possible WTs, and these progenies would all segregate 100% standard *Hsf1*/+. The

second class would come from sib crossing the *Hsf1*/+ plants heterozygous for the enhancer allele to all possible WTs, resulting in three segregation types, (1) 100% standard *Hsf1*/+, (2) 3 standard *Hsf1*:1 enhanced *Hsf1*, and (3) 1 standard *Hsf1*:1 enhanced *Hsf1*. As expected, at least one of each segregating class was seen for each of the 19 sib crosses performed [Table 8].

Possible linkage to *tru1*

Sib crossing between [*Hsf1*/+, *tru1*/+] x [+/+, *tru1*/+] plants produced six segregating genotypes for the *Hsf1* population [Figure 28]. The population segregated the expected number of wild-type, standard*Hsf1*/+ and enhanced *Hsf1*/+ - which were discarded. For the WT class, I observed the expected 1:2:1 for segregation of *tru1* based on my genotyping assay. However, within the *Hsf1*/+ population I found there were a significant number of *Hsf1*/+, *tru1* double mutant plants absent [Table 8]. Chi-square analysis indicated that *tru1* did indeed segregate 1:2:1, but with such few plants, I failed to recover any *bona fide Hsf1*/+, *tru1*/*tru1* double mutants. Since I did not include the enhanced *Hsf1* plants in the genotyping assay due to severely stunted growth or mortality, I hypothesized that this contributed to my lack of recovering *Hsf1 tru1* doubles. Based on these small numbers, I did not find any linkage between the enhancer and *tru1*.

Discussion

My last objective provides an exciting novel discovery of an enhancer locus to *Hsf1*/+ found in the A619 inbred background. Utilizing eight seed sources, I have data that supports the hypothesis that the genetic enhancer is a recessive locus that interacts with *Hsf1*/+. Several standard *Hsf1* to WT sibs showed different 3:1 and 1:1 segregation ratios of standard vs. enhanced *Hsf1,* supporting my hypothesis. Further analysis using a second progeny test, provided evidence that the enhancer phenotype could be segregated away. This suggests that the enhancer locus did segregate recessively in the first progeny test.

Continuation of the double mutant analysis for *tru1* mutants produced a possible linkage to the enhancer allele. This is due to the *Hsf1*/+ introgression into the *tru1* within the A619 inbred line, producing enhanced plants in the progeny. Since the enhanced plants are sterile in the greenhouse and 100% mortality in the field, we did not maintain these plants. The absence of the enhancer plants from my analysis suggested a possible linkage between *tru1* and the enhancer locus but chi-square analysis failed to support this idea.

Future Directions

Map-based Cloning

The enhanced locus needs to undergo map-based cloning to reveal the underlying gene that accounts for the observed phenotype. There is a possibility that the gene could be a Type-A response regulator that shows similar phenotypes for the *Hsf1/+, abphyl1/abphyl1* mutant. It is also possible that *ZmRR5* is a candidate gene, another Type-A, leading to the notion that the enhanced phenotypes are due to reduced negative regulation of CK signaling. Since I was able to segregate away the enhancer allele, introgression of mutants into this line can now be done with other mutants in the A619 background.

Figure Legends

Figure 25. Possible genetic enhancer in A619 inbred line. Emerging leaf 4 seedlings of wild-type, standard *Hsf1*/+, enhanced *Hsf1*/+ plants. Below each plant are the segregation percentages (red values) of each genotype within the same population. White scale bar is 4 cm.

Figure 26. Enhanced *Hsf1*/+ plants produced phenotypes similar to *aberrant phyllotaxy1* (*abph1*) mutants. Picture is of two seedlings at different developmental stages from the *Hsf1*/+ study in the A619 inbred background. Both show the altered phyllotaxy phenotype.

Figure 27. Expected segregation ratios if the *Hsf1* enhancer is due to a single recessive locus. Initial cross between standard *Hsf1* and A619 inbred line maintained the enhancer allele and proved that the mutation is not fixed. Standard *Hsf1* was sib crossed (red dotted line) to each wild-type genotype. Expected segregation ratios are shown for standard vs. enhanced *Hsf1* plants, either a 3:1 or 1:1.

Figure 28. Phenotypes of the enhanced *Hsf1* plants. Dissection of tubular leaves obtained from the enhanced plants at 10X magnification. (A) picture is before dissecting and (B) is after. Both pictures show the failure for margins to separate. (C)Twin seedling sample taken from an enhanced plant. Image shows the two shoots share same root system and are not twin embryos. Magnification is at 15X.

Figure 29. Validation of single recessive locus hypothesis using a second segregation model. Using progeny that segregated 3:1, standard *Hsf1* crossed to the wild-type sibs creates several segregating classes. The six expected progeny segregations within the *Hsf1* population are shown above.

Figures

Figure 24. Possible genetic enhancer in A619 inbred line. Emerging leaf 4 seedlings of wild-type, standard *Hsf1/+,* enhanced *Hsf1/+* plants. Below each plant are the segregation percentages (red values) of each genotype within the same population. White scale bar is 4 cm.

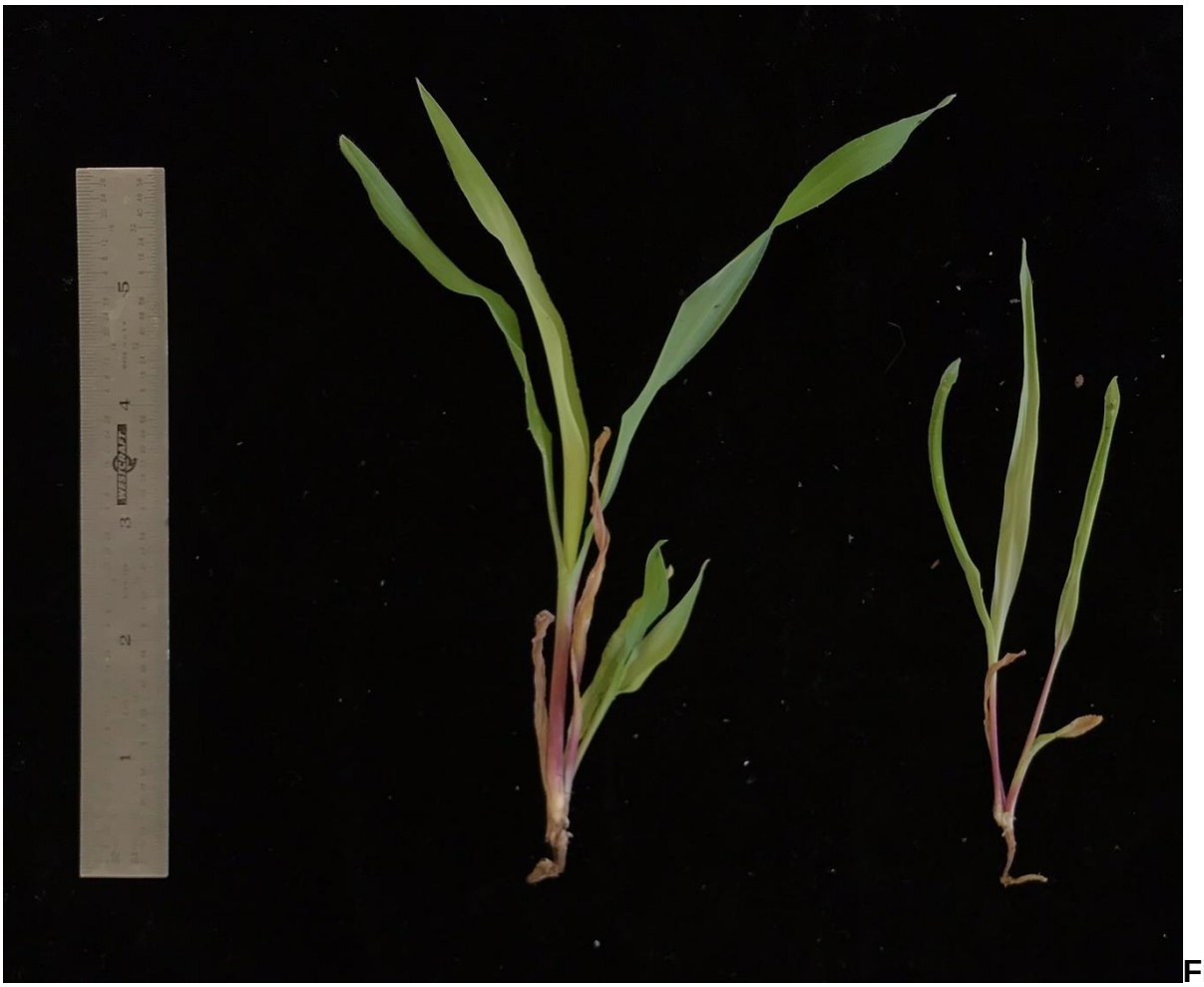

Figure 25. Enhanced *Hsf1/+* plants produced phenotypes similar to *aberrant phyllotaxy1* (*abph1*) mutants. Picture is of two seedlings at different developmental stages from the *Hsf1/+* study in the A619 inbred background. Both show the altered phyllotaxy phenotype.

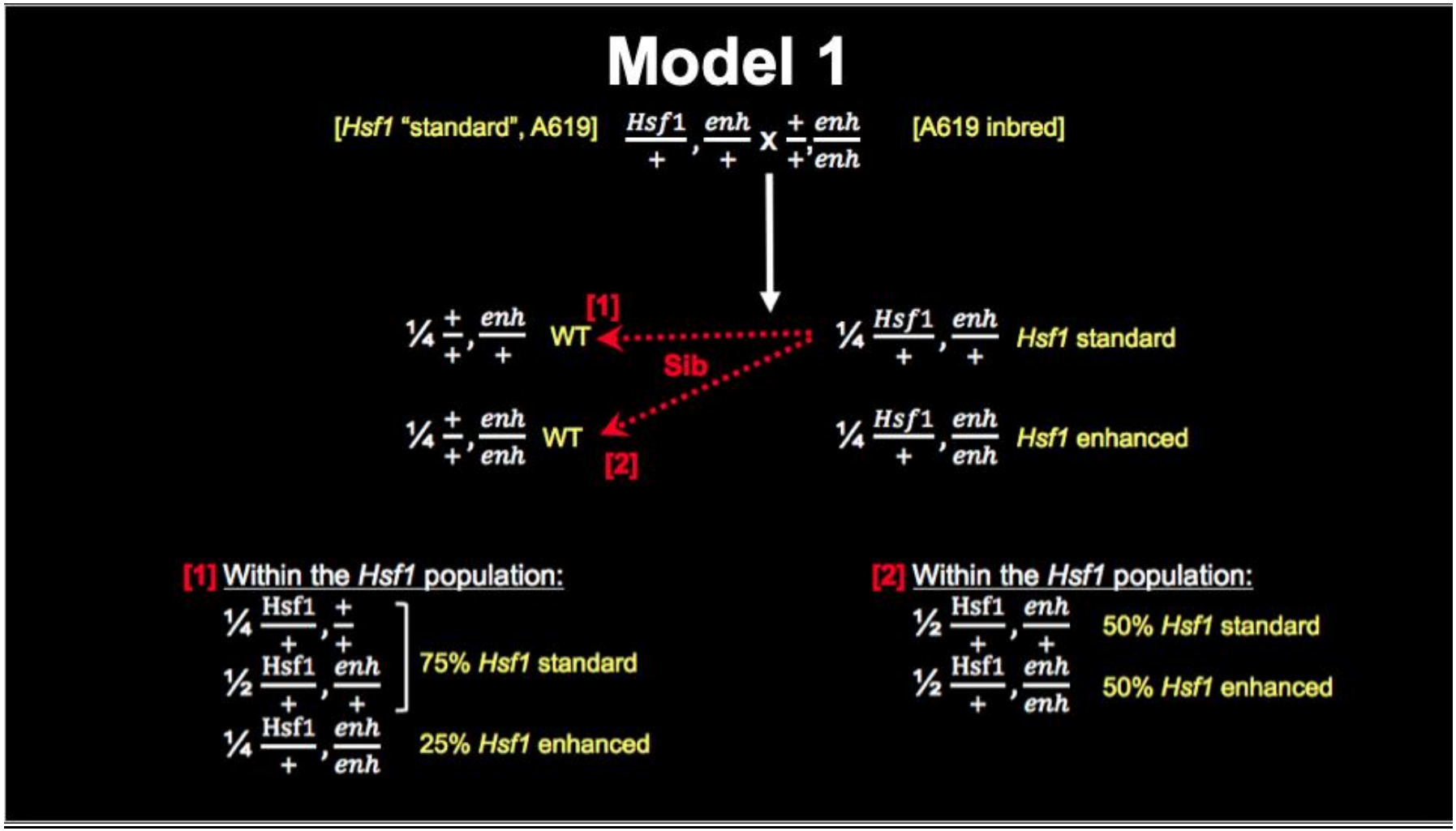

Figure 26. Expected segregation ratios if the *Hsf1* enhancer is due to a single recessive locus. Initial cross between standard *Hsf1* and A619 inbred line maintained the enhancer allele and proved that the mutation is not fixed. Standard *Hsf1* was sib crossed (red dotted line) to each wild-type genotype. Expected segregation ratios are shown for standard vs. enhanced *Hsf1* plants, either a 3:1 or 1:1.

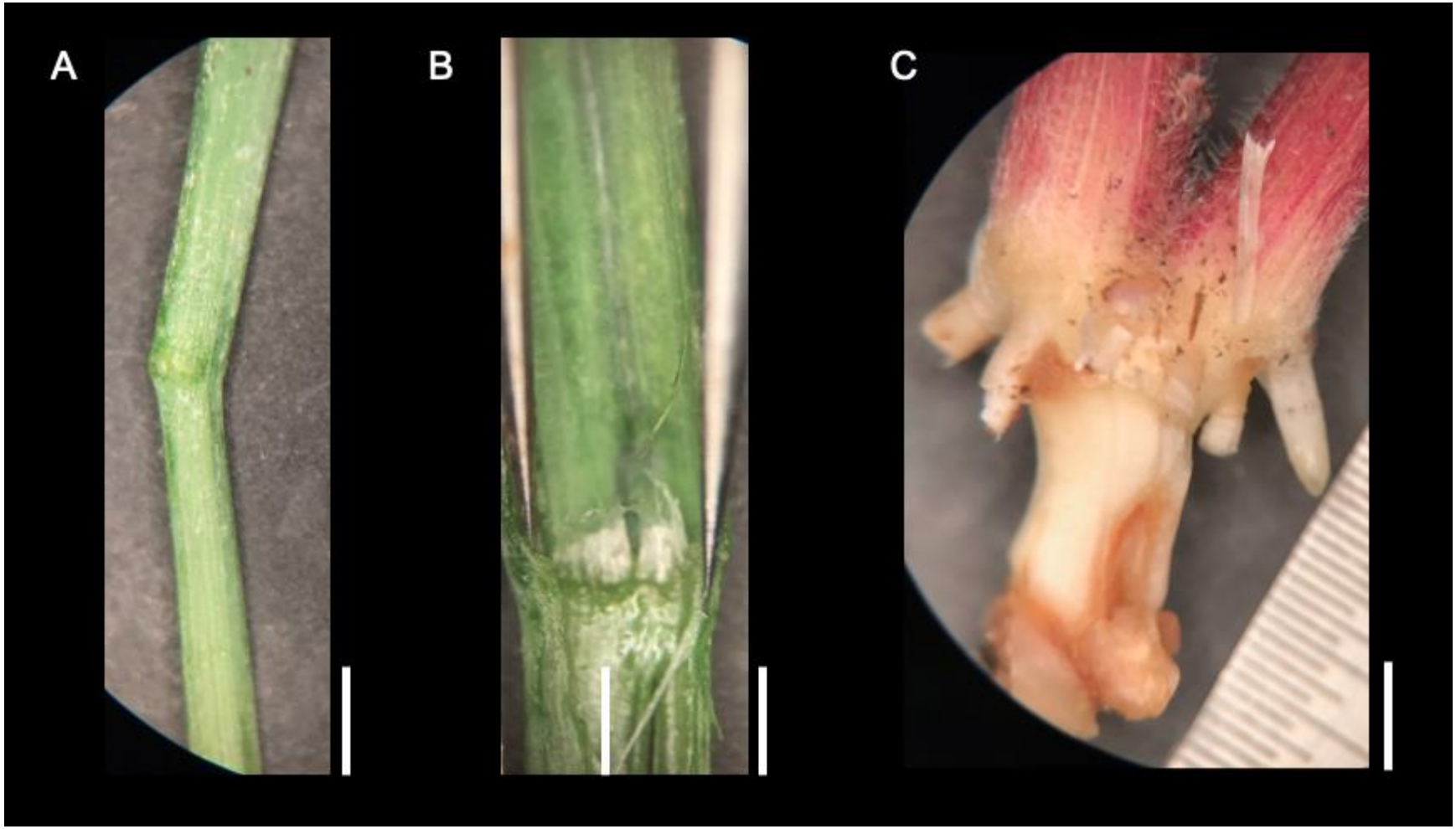

Figure 27. Phenotypes of the enhanced *Hsf1* plants. Dissection of tubular leaves obtained from the enhanced plants at 10X magnification. (A) picture is before dissecting and (B) is after. Both pictures show the failure for margins to separate. (C)Twin seedling sample taken from an enhanced plant. Image shows the two shoots share same root system and are not twin embryos. Magnification is at 15X.

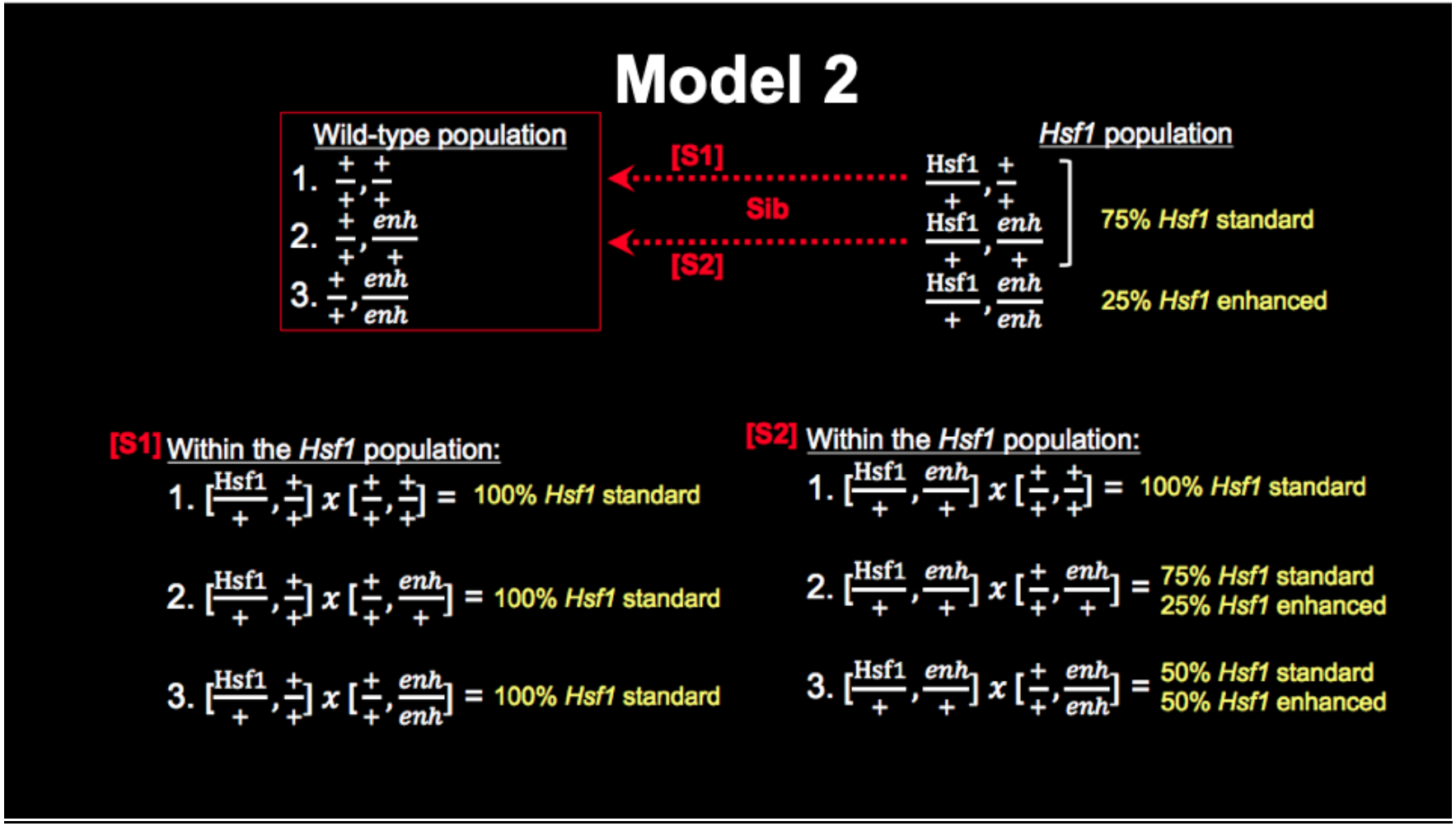

Figure 28. Validation of single recessive locus hypothesis using a second segregation model. Using progeny that segregated 3:1, standard *Hsf1* crossed to the wild-type sibs creates several segregating classes. The six expected progeny segregations within the *Hsf1* population are shown above.

Tables

Source ID	Fem. Plant	Fem. ID	Male Plant	Male ID	1:1	3:1
GYN0040	Hsf1	11	Wt	2	**0.285**	0.001
GYN0041	Hsf1	12	Wt	1	**0.819**	0.024
GYN0042	Hsf1	12	Wt	5	**0.052**	0.000
GYN0043	Hsf1	11	Wt	8	**0.491**	0.001
GYN0044	Hsf1	12	Wt	6	**0.317**	0.037
GYN0047	Hsf1	13	Wt	14	**0.090**	**0.674**
GYN0048	Wt	5	Hsf1	12	0.002	**0.150**
GYN0049	Wt	14	Hsf1	13	**0.052**	**0.873**

Table 7. Segregation results of the 8 progeny sib crosses from Model 1. Above shows the female and male phenotypes used in each cross. Last two columns are a chi-square result of the observed enhanced to standard *Hsf1* plants. P≥ 0.5 are in bold and follow the expected segregation ratio.

Seed Source	# of WT	# of Sta.	# of Enh.	1:1	3:1
GYN0070	18	10	3	1.00	0.15
GYN0071	18	9	5	0.40	0.45
GYN0072	7	15	-	-	-
GYN0073	13	7	9	0.03	0.48
GYN0074	6	4	1	1.00	0.30
GYN0075	18	7	7	0.12	1.00
GYN0076	25	7	-	-	-
GYN0077	15	7	6	0.17	0.84
GYN0078	12	9	9	0.08	1.00
GYN0079	14	4	13	0.00	0.11
GYN0081	15	8	6	0.22	0.70
GYN0082	5	2	4	0.09	0.56
GYN0083	13	13	5	0.70	0.17
GYN0084	10	15	6	0.73	0.15
GYN0085	15	11	5	0.69	0.28
GYN0086	17	6	8	0.05	0.70
GYN0087	14	7	9	0.07	0.72
GYN0088 (1st)	16	6	8	0.04	0.55
GYN0088 (2nd)	18	7	5	0.39	0.68

Table 8. Chi-square results of second progeny test. First column is the seed source. Second, third, and fourth column are the number of observed plants for each phenotype. Last two columns are the calculated p-values for a 1:1 and 3:1 (standard: enhanced) *Hsf1* segregation ratio. Standard confidence; $P \leq 0.05$. WT, wild-type; Sta., Standard *Hsf1*; Enh., Enhanced *Hsf1.*

REFERENCES

Aimee Naomi Uyehara. (2018). *Characterizing a novel connection between the plant hormones cytokinin and jasmonic acid in control of maize leaf growth*. 66.

Atwell, B. J. (Brian J., Kriedemann, P. E., & Turnbull, C. G. N. (1999). *Plants in action : adaptation in nature, performance in cultivation*. Retrieved from https://books.google.com/books/about/Plants_in_Action.html?id=chWs4ewSzpEC

Bauer, P., Lubkowitz, M., Tyers, R., Nemoto, K., Meeley, R. B., Goff, S. A., & Freeling, M. (2004). Regulation and a conserved intron sequence of liguleless3/4 knox class-I homeobox genes in grasses. *Planta*, *219*(2), 359–368. https://doi.org/10.1007/s00425-004-1233-6

Bertrand-Garcia, R., & Freeling, M. (1991). Hairy-sheath frayed #1-O: a systemic, heterochronic mutant of maize that specifies slow developmental stage transitions. *American Journal of Botany*, *78*(6), 747–765. https://doi.org/10.1002/j.1537-2197.1991.tb14477.x

Bishopp, A., Lehesranta, S., Vatén, A., Help, H., El-Showk, S., Scheres, B., … Helariutta, Y. (2011). Phloem-Transported Cytokinin Regulates Polar Auxin Transport and Maintains Vascular Pattern in the Root Meristem. *Current Biology*, *21*(11), 927–932. https://doi.org/10.1016/J.CUB.2011.04.049

Bolle, C. (2004). The role of GRAS proteins in plant signal transduction and development. *Planta*, *218*(5), 683–692. https://doi.org/10.1007/s00425-004-1203-z

Borzouei, A., Kafi, M., Khazaei, H., Naeriyan, B., & A.Majdabadi. (2010). Effects of Gamma Radiation on Germination and Physiological Aspects of Wheat. *Pak J Bot*, *42*(4), 2281–2290.

Cahill, J. F. (2015). Analysis of cytokinin-induced maize leaf developmental changes and interacting genetic modifiers. *Graduate Theses and Dissertations*, *1*. https://doi.org/10.1017/CBO9781107415324.004

Chandler, J. W., & Werr, W. (2015). Cytokinin–auxin crosstalk in cell type specification. *Trends in Plant Science*, *20*(5), 291–300. https://doi.org/10.1016/J.TPLANTS.2015.02.003

Chen, C. (1997). Cytokinin biosynthesis and interconversion. *Physiologia Plantarum*, *101*(4), 665–673. https://doi.org/10.1111/j.1399-3054.1997.tb01051.x

D'Aloia, M., Bonhomme, D., Bouché, F., Tamseddak, K., Ormenese, S., Torti, S., … Périlleux, C. (2011). Cytokinin promotes flowering of Arabidopsis via transcriptional activation of the FT paralogue TSF. *Plant Journal*, *65*(6), 972–979. https://doi.org/10.1111/j.1365-313X.2011.04482.x

Dello Ioio, R., Linhares, F. S., Scacchi, E., Casamitjana-Martinez, E., Heidstra, R., Costantino, P., & Sabatini, S. (2007). Cytokinins Determine Arabidopsis Root-Meristem Size by Controlling Cell Differentiation. *Current Biology*, *17*(8), 678–682. https://doi.org/10.1016/J.CUB.2007.02.047

Dong, Z., Li, W., Unger-Wallace, E., Yang, J., Vollbrecht, E., & Chuck, G. (2017). Ideal crop plant architecture is mediated by tassels replace upper ears1, a BTB/POZ ankyrin repeat gene directly targeted by TEOSINTE BRANCHED1. *Proceedings of the National Academy of Sciences of the United States of America*, *114*(41), E8656–E8664. https://doi.org/10.1073/pnas.1714960114

Englbrecht, C. C., Schoof, H., & Böhm, S. (2004). Conservation, diversification and expansion of C2H2 zinc finger proteins in the Arabidopsis thaliana genome. *BMC Genomics*, *5*(1), 39. https://doi.org/10.1186/1471-2164-5-39

Freytag, A. H., Rao-Arelli, A. P., Anand, S. C., Wrather, J. A., & Owens, L. D. (1989). Somaclonal variation in soybean plants regenerated from tissue culture. *Plant Cell Reports*, *8*(4), 199–202. https://doi.org/10.1007/BF00778531

GENEWIZ - SOLID SCIENCE. SUPERIOR SERVICE. (n.d.). Retrieved August 7, 2019, from https://www.genewiz.com/en

Giulini, A., Wang, J., & Jackson, D. (2004). Control of phyllotaxy by the cytokinin-inducible response regulator homologue ABPHYL1. *Nature*, *430*(7003), 1031–1034. https://doi.org/10.1038/nature02778

Gordon, S. P., Chickarmane, V. S., Ohno, C., & Meyerowitz, E. M. (2009). Multiple feedback loops through cytokinin signaling control stem cell number within the Arabidopsis shoot meristem. *Proceedings of the National Academy of Sciences of the United States of America*, *106*(38), 16529–16534. https://doi.org/10.1073/pnas.0908122106

Han, Y., Yang, H., & Jiao, Y. (2014). Regulation of inflorescence architecture by cytokinins. *Frontiers in Plant Science*, *5*, 669. https://doi.org/10.3389/fpls.2014.00669

Hanway, J. J. (1966). How a corn plant develops. *Special Report*. Retrieved from http://www.sidalc.net/cgi-bin/wxis.exe/?IsisScript=UACHBC.xis&method=post&formato=2&cantidad=1&expresion=mfn=014100

Hareven, D., Gutfinger, T., Parnis, A., Eshed, Y., & Lifschitz, E. (1996). The Making of a Compound Leaf: Genetic Manipulation of Leaf Architecture in Tomato. *Cell*, *84*(5), 735–744. https://doi.org/10.1016/S0092-8674(00)81051-X

Hopkins, W. G., & Hüner, N. P. A. (2008). *Introduction to plant physiology*. Retrieved from https://www.wiley.com/en-us/Introduction+to+Plant+Physiology%2C+4th+Edition-p-9780470247662

Ikeda, M., & Ohme-Takagi, M. (2014). TCPs, WUSs, and WINDs: families of transcription factors that regulate shoot meristem formation, stem cell maintenance, and somatic cell differentiation. *Frontiers in Plant Science*, *5*, 427. https://doi.org/10.3389/fpls.2014.00427

Inoue, T., Higuchi, M., Hashimoto, Y., Seki, M., Kobayashi, M., Kato, T., … Kakimoto, T. (2001). Identification of CRE1 as a cytokinin receptor from Arabidopsis. *Nature*, *409*(6823), 1060–1063. https://doi.org/10.1038/35059117

Iuchi, S. (2001). Three classes of C2H2 zinc finger proteins. *Cellular and Molecular Life Sciences*, *58*(4), 625–635. https://doi.org/10.1007/PL00000885

Iwase, A., Mitsuda, N., Koyama, T., Hiratsu, K., Kojima, M., Arai, T., … Ohme-Takagi, M. (2011). The AP2/ERF Transcription Factor WIND1 Controls Cell Dedifferentiation in Arabidopsis. *Current Biology*, *21*(6), 508–514. https://doi.org/10.1016/J.CUB.2011.02.020

Iwase, A., Ohme-Takagi, M., & Sugimoto, K. (2011). WIND1. *Plant Signaling & Behavior*, *6*(12), 1943–1945. https://doi.org/10.4161/psb.6.12.18266

Izumi, K., Nakagawa, S., Kobayashi, M., Oshio, H., Sakurai, A., & Takahashi, N. (1988). Levels of IAA, Cytokinins, ABA and Ethylene in Rice Plants as Affected by a

Gibberellin Biosynthesis Inhibitor, Uniconazole-P. *Plant and Cell Physiology*, *29*(1), 97–104. https://doi.org/10.1093/oxfordjournals.pcp.a077480
Johnston, R., Wang, M., Sun, Q., Sylvester, A. W., Hake, S., & Scanlon, M. J. (2014). Transcriptomic Analyses Indicate That Maize Ligule Development Recapitulates Gene Expression Patterns That Occur during Lateral Organ Initiation. *The Plant Cell Online*, *26*(12), 4718–4732. https://doi.org/10.1105/tpc.114.132688
Kang, J., Lee, Y., Sakakibara, H., & Martinoia, E. (2017). Cytokinin Transporters: GO and STOP in Signaling. *Trends in Plant Science*, *22*(6), 455–461. https://doi.org/10.1016/J.TPLANTS.2017.03.003
Kessler, S., & Sinha, N. (2004). Shaping up: the genetic control of leaf shape. *Current Opinion in Plant Biology*, *7*(1), 65–72. https://doi.org/10.1016/J.PBI.2003.11.002
Kyozuka, J. (2007). Control of shoot and root meristem function by cytokinin. *Current Opinion in Plant Biology*, *10*(5), 442–446. https://doi.org/10.1016/J.PBI.2007.08.010
Lee, B., Johnston, R., Yang, Y., Gallavotti, A., Kojima, M., Travençolo, B. A. N., … Jackson, D. (2009). Studies of aberrant phyllotaxy1 mutants of maize indicate complex interactions between auxin and cytokinin signaling in the shoot apical meristem. *Plant Physiology*, *150*(1), 205–216. https://doi.org/10.1104/pp.109.137034
Leibfried, A., To, J. P. C., Busch, W., Stehling, S., Kehle, A., Demar, M., … Lohmann, J. U. (2005). WUSCHEL controls meristem function by direct regulation of cytokinin-inducible response regulators. *Nature*, *438*(7071), 1172–1175. https://doi.org/10.1038/nature04270
Letham, D. S. (1963). Zeatin, a factor inducing cell division isolated from Zea mays. *Life Sciences*, *2*(8), 569–573. https://doi.org/10.1016/0024-3205(63)90108-5
Lewis, M. W., Bolduc, N., Hake, K., Htike, Y., Hay, A., Candela, H., & Hake, S. (2014). Gene regulatory interactions at lateral organ boundaries in maize. *Development (Cambridge, England)*, *141*(23), 4590–4597. https://doi.org/10.1242/dev.111955
Li, M., Tang, D., Wang, K., Wu, X., Lu, L., Yu, H., … Cheng, Z. (2011). Mutations in the F-box gene LARGER PANICLE improve the panicle architecture and enhance the grain yield in rice. *Plant Biotechnology Journal*, *9*(9), 1002–1013. https://doi.org/10.1111/j.1467-7652.2011.00610.x
Liu, J., Moore, S., Chen, C., & Lindsey, K. (2017). Crosstalk Complexities between Auxin, Cytokinin, and Ethylene in Arabidopsis Root Development: From Experiments to Systems Modeling, and Back Again. *Molecular Plant*, *10*(12), 1480–1496. https://doi.org/10.1016/J.MOLP.2017.11.002
MacArthur, L. A., & D'Appolonia, B. . (1984). *Gamma Radiation of Wheat. II. Effects of Low-Dosage Radiations on Starch Properties*. Retrieved from https://www.aaccnet.org/publications/cc/backissues/1984/Documents/Chem61_321.pdf
Machida, C., Nakagawa, A., Kojima, S., Takahashi, H., & Machida, Y. (2015). The complex of ASYMMETRIC LEAVES (AS) proteins plays a central role in antagonistic interactions of genes for leaf polarity specification in Arabidopsis. *Wiley Interdisciplinary Reviews: Developmental Biology*, *4*(6), 655–671. https://doi.org/10.1002/wdev.196
Manoli, A., Sturaro, A., Trevisan, S., Quaggiotti, S., & Nonis, A. (2012). Evaluation of candidate reference genes for qPCR in maize. *Journal of Plant Physiology*, *169*(8),

807–815. https://doi.org/10.1016/J.JPLPH.2012.01.019
Moon, J., Candela, H., & Hake, S. (2013). The Liguleless narrow mutation affects proximal-distal signaling and leaf growth. *Development (Cambridge, England)*, *140*(2), 405–412. https://doi.org/10.1242/dev.085787
Moubayidin, L., Di Mambro, R., & Sabatini, S. (2009). Cytokinin–auxin crosstalk. *Trends in Plant Science*, *14*(10), 557–562. https://doi.org/10.1016/J.TPLANTS.2009.06.010
Muehlbauer, G. J., Fowler, J. E., Girard, L., Tyers, R., Harper, L., & Freeling, M. (1999). Ectopic Expression of the Maize Homeobox Gene Liguleless3 Alters Cell Fates in the Leaf. *Plant Physiology*, *119*(2), 651–662. https://doi.org/10.1104/pp.119.2.651
Muszynski, M. G., Dam, T., Li, B., Shirbroun, D. M., Hou, Z., Bruggemann, E., … Danilevskaya, O. N. (2006). Delayed flowering1 Encodes a basic leucine zipper protein that mediates floral inductive signals at the shoot apex in maize. *Plant Physiology*, *142*(4), 1523–1536. https://doi.org/10.1104/pp.106.088815
Muthamilarasan, M., Bonthala, V. S., Mishra, A. K., Khandelwal, R., Khan, Y., Roy, R., & Prasad, M. (2014). C2H2 type of zinc finger transcription factors in foxtail millet define response to abiotic stresses. *Functional & Integrative Genomics*, *14*(3), 531–543. https://doi.org/10.1007/s10142-014-0383-2
Pautler, M., Tanaka, W., Hirano, H.-Y., & Jackson, D. (2013). Grass Meristems I: Shoot Apical Meristem Maintenance, Axillary Meristem Determinacy and the Floral Transition. *Plant and Cell Physiology*, *54*(3), 302–312. https://doi.org/10.1093/pcp/pct025
Pilkington, S. M., Montefiori, M., Galer, A. L., Neil Emery, R. J., Allan, A. C., & Jameson, P. E. (2013). Endogenous cytokinin in developing kiwifruit is implicated in maintaining fruit flesh chlorophyll levels. *Annals of Botany*.
Pritchard, G. I., Pigden, W. J., & Minson, D. J. (1962). EFFECT OF GAMMA RADIATION ON THE UTILIZATION OF WHEAT STRAW BY RUMEN MICROORGANISMS. *Canadian Journal of Animal Science*, *42*(2), 215–217. https://doi.org/10.4141/cjas62-033
Ramirez, J., Bolduc, N., Lisch, D., & Hake, S. (2009). Distal Expression of knotted1 in Maize Leaves Leads to Reestablishment of Proximal/Distal Patterning and Leaf Dissection. *PLANT PHYSIOLOGY*, *151*(4), 1878–1888. https://doi.org/10.1104/pp.109.145920
Richardson, A., & Hake, S. (2018). Drawing a Line: Grasses and Boundaries. *Plants*, *8*(1), 4. https://doi.org/10.3390/plants8010004
Rodo, A. P., Brugière, N., Vankova, R., Malbeck, J., Olson, J. M., Haines, S. C., … Mok, M. C. (2008). Over-expression of a zeatin O-glucosylation gene in maize leads to growth retardation and tasselseed formation. *Journal of Experimental Botany*, *59*(10), 2673–2686. https://doi.org/10.1093/jxb/ern137
Saberman, J., & Bertrand-Garcia, R. (1997). Hairy-sheath-frayed 1–O is a Non-Cell-Autonomous Mutation That Regulates Developmental Stage Transitions in Maize. *Journal of Heredity*, *88*(6), 549–553. https://doi.org/10.1093/oxfordjournals.jhered.a023157
Sacristan, M. D., & Melchers, G. (1969). The caryological analysis of plants regenerated from tumorous and other callus cultures of tobacco. *MGG Molecular & General Genetics*, *105*(4), 317–333. https://doi.org/10.1007/BF00277587
Sakakibara, H. (2006). CYTOKININS: Activity, Biosynthesis, and Translocation. *Annual*

Review of Plant Biology, *57*(1), 431–449. https://doi.org/10.1146/annurev.arplant.57.032905.105231

Sankar, M., Osmont, K. S., Rolcik, J., Gujas, B., Tarkowska, D., Strnad, M., … Hardtke, C. S. (2011). A qualitative continuous model of cellular auxin and brassinosteroid signaling and their crosstalk. *Bioinformatics*, *27*(10), 1404–1412. https://doi.org/10.1093/bioinformatics/btr158

Scanlon, M. J., Schneeberger, R. G., Freeling, M., & Jurgens, G. (1996). The maize mutant narrow sheath fails to establish leaf margin identity in a meristematic domain. *Development (Cambridge, England)*, *122*(6), 1683–1691. Retrieved from http://www.ncbi.nlm.nih.gov/pubmed/8674408

Schaller, G. E., Bishopp, A., & Kieber, J. J. (2015). The yin-yang of hormones: cytokinin and auxin interactions in plant development. *The Plant Cell*, *27*(1), 44–63. https://doi.org/10.1105/tpc.114.133595

Schmittgen, T. D., & Livak, K. J. (2008). Analyzing real-time PCR data by the comparative CT method. *Nature Protocols*, *3*(6), 1101–1108. https://doi.org/10.1038/nprot.2008.73

Schmülling, T., Werner, T., Riefler, M., Krupková, E., & Bartrina y Manns, I. (2003). Structure and function of cytokinin oxidase/dehydrogenase genes of maize, rice, Arabidopsis and other species. *Journal of Plant Research*, *116*(3), 241–252. https://doi.org/10.1007/s10265-003-0096-4

Shen, Q., Wang, Y.-T., Tian, H., & Guo, F.-Q. (2013). Nitric Oxide Mediates Cytokinin Functions in Cell Proliferation and Meristem Maintenance in Arabidopsis. *Molecular Plant*, *6*(4), 1214–1225. https://doi.org/10.1093/MP/SSS148

Skalák, J., Vercruyssen, L., Claeys, H., Hradilová, J., Černý, M., Novák, O., … Brzobohatý, B. (2019). Multifaceted activity of cytokinin in leaf development shapes its size and structure in Arabidopsis. *The Plant Journal : For Cell and Molecular Biology*, *97*(5), 805–824. https://doi.org/10.1111/tpj.14285

SKOOG, F., & MILLER, C. O. (1957). Chemical regulation of growth and organ formation in plant tissues cultured in vitro. *Symposia of the Society for Experimental Biology*, *11*, 118–130. Retrieved from http://www.ncbi.nlm.nih.gov/pubmed/13486467

Su, Y. H., Liu, Y. B., & Zhang, X. S. (2011). Auxin-cytokinin interaction regulates meristem development. *Molecular Plant*, Vol. 4, pp. 616–625. https://doi.org/10.1093/mp/ssr007

TAKAGI, M., YOKOTA, T., MUROFUSHI, N., OTA, Y., & TAKAHASHI, N. (1985). Fluctuation of endogenous cytokinin contents in rice during its life cycle. Quantification of cytokinins by selected ion monitoring using deuterium-labelled internal standards. *Agricultural and Biological Chemistry*, *49*(11), 3271–3277. https://doi.org/10.1271/bbb1961.49.3271

Takagi, M., Yokota, T., Murofushi, N., Saka, H., & Takahashi, N. (1989). Quantitative changes of free-base, riboside, ribotide and glucoside cytokinins in developing rice grains. *Plant Growth Regulation*, *8*(4), 349–364. https://doi.org/10.1007/BF00024665

Takei, K., Yamaya, T., & Sakakibara, H. (2004). Arabidopsis CYP735A1 and CYP735A2 encode cytokinin hydroxylases that catalyze the biosynthesis of trans-Zeatin. *The Journal of Biological Chemistry*, *279*(40), 41866–41872.

https://doi.org/10.1074/jbc.M406337200
Toriba, T., Tokunaga, H., Shiga, T., Nie, F., Naramoto, S., Honda, E., … Kyozuka, J. (2019a). BLADE-ON-PETIOLE genes temporally and developmentally regulate the sheath to blade ratio of rice leaves. *Nature Communications*, *10*(1). https://doi.org/10.1038/s41467-019-08479-5
Toriba, T., Tokunaga, H., Shiga, T., Nie, F., Naramoto, S., Honda, E., … Kyozuka, J. (2019b). BLADE-ON-PETIOLE genes temporally and developmentally regulate the sheath to blade ratio of rice leaves. *Nature Communications*, *10*(1), 619. https://doi.org/10.1038/s41467-019-08479-5
Townsley, B. T., Sinha, N. R., & Kang, J. (2013). KNOX1 genes regulate lignin deposition and composition in monocots and dicots. *Frontiers in Plant Science*, *4*. https://doi.org/10.3389/fpls.2013.00121
Veit, B., Schmidt, R. J., Hake, S., Yanofsky, M. F., Hake, S., & Yanofsky, M. F. (1993). Maize Floral Development: New Genes and Old Mutants. *THE PLANT CELL ONLINE*, *5*(10), 1205–1215. https://doi.org/10.1105/tpc.5.10.1205
Wybouw, B., & De Rybel, B. (2019). Cytokinin – A Developing Story. *Trends in Plant Science*, *24*(2), 177–185. https://doi.org/10.1016/J.TPLANTS.2018.10.012
Yanai, O., Shani, E., Dolezal, K., Tarkowski, P., Sablowski, R., Sandberg, G., … Ori, N. (2005). Arabidopsis KNOXI proteins activate cytokinin biosynthesis. *Current Biology*, *15*(17), 1566–1571. https://doi.org/10.1016/j.cub.2005.07.060
Zhang, K., Letham, D., & John, P. L. (1996). Cytokinin controls the cell cycle at mitosis by stimulating the tyrosine dephosphorylation and activation of p34cdc2-like H1 histone kinase. *Planta*, *200*(1), 2–12. https://doi.org/10.1007/BF00196642
Zimmermann, R., & Werr, W. (2005). Pattern Formation in the Monocot Embryo as Revealed by NAMand CUC3 Orthologues from Zea mays L. *Plant Molecular Biology*, *58*(5), 669–685. https://doi.org/10.1007/s11103-005-7702-x